EUROPEAN ORGANIZATION FOR NUCLEAR RESEARCH

CERN/PS 92-23 (HI)
7 April 1992

ION SOURCES

Helmut Haseroth and Heinrich Hora
CERN,
Geneva, Switzerland

To be published in New Methods and Technologies,
Chapter IV of *Advances of Accelerator Physics and Technologies*,
ed. Herwig Schopper, World Scientific Publishing Company, Singapore.

ION SOURCES

Helmut Haseroth and Heinrich Hora,
CERN,
Geneva, Switzerland

ABSTRACT

Ion sources for accelerators are based on plasma configurations with an extraction system in order to gain a very high number of ions within an appropriately short pulse and of sufficiently high charge number Z for advanced research. Beginning with the duoplasmatron, all established ion sources are based on low-density plasmas, of which the electron beam ionization source (EBIS) and the electron cyclotron resonance (ECR) source are the most advanced; for example they result in pulses of nearly 6×10^8 fully stripped sulfur ions per pulse in the Super Proton Synchrotron (SPS) at CERN with energies of 200 GeV/u. As an example of a forthcoming development, we are reporting about the lead ion source for the same purpose. Contrary to these cases of low-density plasmas, where a rather long time is always necessary to generate sufficiently high charge states, the laser ion source uses very high density plasmas and therefore produced, for example in 1983, single shots of Au^{51+} ions of high directivity with energies above 300 MeV within 2 ns irradiation time of a gold target with a medium-to-large CO_2 laser. Experiments at Dubna and Moscow, using small-size lasers, produced up to one million shots with 1 Hz sequence. After acceleration by a linac or otherwise, ion pulses of up to nearly 5×10^{10} ions of C^{4+} or Mg^{12+} with energies in the synchrotrons of up to 2 GeV/u were produced. The physics of the laser generation of the ions is most complex, as we know from laser fusion studies, including non-linear dynamic and dielectric effects, resonances, self-focusing, instabilities, double layers, and an irregular pulsation in the 20 ps range. This explains not only what difficulties are implied with the laser ion source, but also why it opens up a new direction of ion sources.

1. Introduction

Ion sources already have a long history. Although in the first real linear accelerator, Wideröe used alkaline ions (Na^+ and K^+), proton sources played the dominant role in the accelerator world.

Protons (and electrons) were quite adequate for elementary particle physics and heavier ions were used only at relatively low energies for nuclear physics. Sometimes

very specialized machines, for example, Unilac at GSI (Darmstadt), were built for this purpose. However, it was obvious that as soon as heavier ions such as deuterons and alpha particles became available in higher energy machines as, for example, the Intersecting Storage Rings (ISR), they were used; and following the high-energy applications of even heavier particles, for example, at GSI and at the Bevalac, the strong demand for relativistic ion beams was successfully met at the BNL Alternating Gradient Synchrotron (AGS) and the CERN Super Proton Synchrotron (SPS). At both accelerator centres a programme is under way (RHIC at BNL and Pb ions for the SPS at CERN) to increase the energy and mass range of the beams. The acceleration of heavy ions to high energies is hampered, of course, by their heavy masses. Hence ion sources which can produce high charge states are desired because it is the charge-to-mass ratio q/m that determines how easily the ions can be accelerated.

The dominant process for producing ions in ion sources is by collisions with sufficiently highly energetic electrons. The first basic problem is how to heat the plasma or at least the electrons; the second is how to extract the ions and how to form a high-quality beam. High quality in this context usually means high current and low emittance.

A typical example for a 'classical' ion source is the duoplasmatron, invented by Manfred von Ardenne[1], where an electrical discharge (arc) is burning in a gas at relatively low pressure in the range of a few 10^{-4} bar (Fig. 1). This discharge is passing through two constrictions: one is of geometrical nature; the other uses a magnetic field of rotational symmetry, focusing the discharge on to a small hole in the anode.

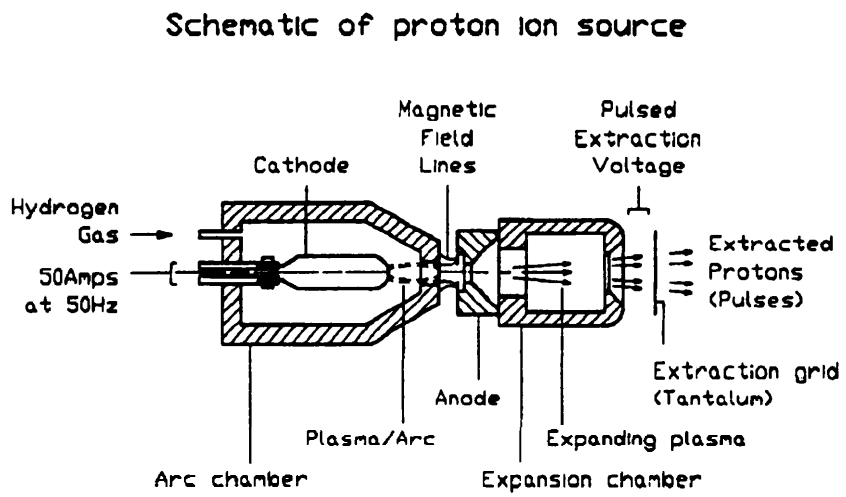

Fig. 1 Advanced version of a duoplasmatron[1]

Through this hole the plasma escapes into the region called the 'expansion cup'. At the end of this cup an electric field is applied to extract the ions. This type of source works very well for low-charge states and light ions.

There is a large variety of ion sources. They differ in the method of heating the plasma (or of the electrons) and in the confinement of the ions. For the heating, different methods are applied: electric discharges, injection of high-energy electrons, RF (including microwave) heating, or (nowadays) heating by laser radiation. For the confinement—if any—different magnetic or electric configurations are used.

Typical arrangements include homogeneous solenoidal fields, or inhomogeneous solenoidal fields with a minimum in the area where the ions should be confined ('mirror machines' or 'minimum-B field configurations'), and confinement with (magnetic) multipole (cusp) fields.

Apart from H^- sources and cluster accelerators, which are used and developed for special applications such as fusion plasma heating or as neutral beam weapons, most of the present-day development is for beams of heavy ions with high-charge states.

Three different types of sources for this application deserve special attention:

- Electron Cyclotron Resonance (ECR) sources
- Electron Beam Ionization Sources (EBIS)
- Laser Ion Sources (LIS).

EBIS and ECR sources are well developed and are in use at several laboratories. Nevertheless, further improvements are certainly possible and research is being actively pursued. Laser ion sources have only started their development with a minimum of resources, both in terms of manpower and money, and are very likely to have a large potential in terms of future improvements. In the following we shall concentrate on these three source types, with emphasis on the last one.

It has been stated that heating and confinement are important characteristics for any ion source. It is obvious that the electrons which are used to ionize the atoms (or further ionize the low-charge-state ions) must have an energy higher than the relevant ionization potential. As a matter of fact, to profit from the largest cross-section, the electrons should have an energy about a factor of three higher. Sufficient energy of the electrons is only one condition for producing ions; the other condition is that there must be a sufficient number of collisions to produce the desired ions. In this context, the concept of the '$n_e\tau$ product' is of importance; n_e stands for the electron density and τ refers to the confinement time. For the EBIS and ECR sources (see Section 2) n_e is small, and hence the confinement time has to be large. For laser ion sources the opposite statement holds: n_e is very large and hence τ can be very short: no special confinement may be needed (see Sections 4 to 6).

In order to illustrate the motivation for using heavy ions in high-energy physics, one example is the forthcoming Large Hadron Collider (LHC). Its design makes it possible to accelerate heavy ions, such as, for example, lead, to energies[2] of 3 TeV/u (624 TeV total ion energy, corresponding to 1248 TeV in an ion–ion collision[2]). Whilst heavy-ion experiments at various places reached a few GeV/u in the past and 15 GeV/u of silicon ions were importantly underlined[2], the CERN SPS has reached 200 GeV/u for sulfur ions, and an extension for lead ions of up to 160 GeV/u is being built.

The branch of high-energy physics which is looking into the very-heavy-nuclei collisions expects several results, not only for the high-temperature excitation of nuclei

now reached, which have 150 MeV temperature[2,4], but also for high-energy physics itself. Whilst the discovery of the W and Z bosons was based on proton–antiproton collisions[5], the electron–positron collisions of the Large Electron–Positron storage ring (LEP) with 50 GeV for each particle led to the mass production of these particles. Until the end of 1991, as many as 4 million Z bosons were produced[6], and LEP is considered as a B-meson factory with the numerous further results obtained strongly confirming the Standard Model[6]. Choosing between the alternatives of lepton colliders, proton colliders such as the Superconducting Super Collider (SSC) and the LHC, and very heavy nucleus colliders, even the last ones (for which purposes the LHC is designed too) may provide the possibility (Grabiak, Soff and Greiner, see Ref. 2) of producing the Higgs boson, the still-missing link of the Standard Model.

More detailed knowledge is expected, from the very-heavy-ion colliders, concerning the transition of hadron matter into quark–gluon plasma[7]. Whilst the generation of much higher temperatures than 150 MeV in nuclei should produce a state where according to a model it is expected that free quarks may appear[2], it seems to be substantiated now how the phase transition from the hadron to the quark–gluon state may occur. This can be seen from the plasma-Fermi model of the surface energy of nuclei[7], where the surface energy (determined by the Fermi energy, defined by the hadron mass) is always less than the internal energy of hadrons confined in a sphere if the density is less than the known value of the nuclear density. Equilibrium appears just at the nuclear density. For densities a little higher (up to about four times, depending on the size of the nucleus), the surface energy is higher than the internal energy by an exponent of only 1/6 for the density. For higher densities, the Fermi energy changes into the relativistic branch and the exponent 1/6 goes to zero. Therefore, for higher densities, any nuclear structure is abolished and, since this relativistic Fermi energy is mass independent, the pure quark–gluon plasma remains as the state in the interior of stars.

What is essential then is the equation of the state of the nucleus[7], which was fundamental[2] in the work of Scheid, Müller and Greiner when studying the shock waves in nuclei[8]. The nuclei are not simply interpenetrating but produce a temperature and a pressure which was measured[2]. Densities up to three times that of the nuclei have been reached with the collisions of very heavy nuclei of energies up to 10 GeV/u [2]. The collisions of nuclei of medium weight, as for example sulfur of 200 GeV/u, seem not to permit sufficient time for establishing the pressures and the shock waves[2]. With the super-relativistic collisions of the very heavy nuclei expected with the LHC, the nuclear densities are expected to reach values sufficient for the phase transition of the hadron matter into the quark–gluon plasma, so that this state can then be studied in detail.

There is no longer any question of the development of the best possible ion sources for this new generation of large accelerators being a negligible part of the development costs, as it was in the past. As an example, it is known that with the best classical techniques extended (by a respectable budget) to the highest possible level are still limited to values of ion pulses at least 30 times below the level desired in the LHC[3].

The question is then: what will cost more, the improvement of the beam by stochastic or electron cooling to bridge the difference of the factor 30 or the introduction of other, perhaps new types, of ion sources to achieve the number 30 (or hopefully a much higher value).

The present contribution examines the existing classical technologies of ion generation for accelerators and indicates their presently planned and expected improvements (Sections 2 and 3). A basically new advancement may be expected by the introduction of the laser ion source, which however has not yet been studied sufficiently to cover the basic physical parameters, and the technological development is not at a stage that an ion source for routine operation could be provided. The first technological steps at Dubna with medium-heavy ion pulses of more than a hundred times higher ion numbers than by using the classical sources have shown new and encouraging aspects. These technologies, however, were performed with small to medium size lasers only and the knowledge of very intense single pulse research of laser-produced plasmas indicates again a very much higher ion number output, and properties of higher energy and directivity than at medium laser operation (Section 4).

The physics of the laser ion source, however, is extremely complex as will be shown in Section 5, and for the moment at least a pragmatic use of some technological properties will be sufficient for the laser ion source (Section 6). In order to appreciate the value of these developments for the new methods and technologies for accelerators, we first need to review the present classical methods. This contribution concentrates on the new methods and technologies and cannot go into all the details of the classical developments. A very comprehensive summary of this work may be found in the book by Ian G. Brown[9], with a number of special articles by the most competent pioneers in the field.

Since practically all ion sources are based on plasmas, we are presenting a diagram with the data found by the various plasma configurations. These values are taken from the book of Brown[9], where the values for the laser fusion and for the laser ion source are added and updated appropriately (Fig. 2). Special attention should be given to the fact that laser-produced plasmas have reached densities in polyethylene of more than one thousand times the solid state[10]; the values are marked with the letter A in the diagram of Fig. 2. The range B is given by a dashed extension only, since the temperatures are that of the 'hot' electrons, and the question may be left aside as to whether this is a real thermal state of the plasma.

2. EBIS and ECR

This section is devoted to the advanced ion sources using 'low' electron densities. It might be mentioned that when ionizing ions by collision with electrons there are basically two possibilities.

The first is to accelerate the ions and to pass them through stationary electrons. This is done, for example, in a stripper foil, which might consist of carbon. Carbon contains about 6.6×10^{23} electrons cm^{-3}. Ions with an energy of, for example,

2 MeV/u are 'confined' in a foil of 1 μm thickness, i.e. they travel through it in a time of 0.5×10^{-13} s. The $n\tau$ product is hence 3×10^{10} cm^{-3} s.

The second possibility is to have the ions (more or less) stationary and to have the electrons accelerated. This is normally the case in ion sources. It is, however, difficult to achieve a high-density of electrons. In an ECR source the typical hot electron density is of the order of 10^{12} cm^{-3}. To achieve an $n\tau$ product of 10^{10} cm^{-3} s therefore requires a confinement time of 10^{-2} s. These values are also typical for an EBIS.

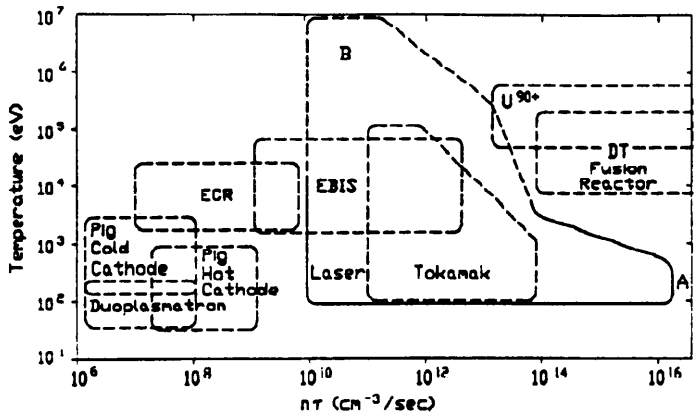

Fig. 2 Products of density n and confinement time τ and temperatures of various plasmas, especially for ion sources, from the results of Brown[9] modified by the results of laser-produced plasmas. (A) refers to the densities of carbohydrates of 1000 times that of the solid reached with lasers[10], and (B) corresponds to the 'hot' electrons (see Fig. 13 of Section 5)

Using semi-empirical formulae[11], the cross-sections to change from charge state q to $q + 1$ can be estimated and the necessary $n\tau$ product calculated.

After its invention at Dubna, development of EBIS has been going on, not only there but also at several other laboratories: Orsay and Saclay, Frankfurt (IAP), Berkeley, and elsewhere. For Saturne (Saclay) an EBIS is used very successfully as injector.

The basic principle of this source is very simple. An electron beam is injected on the axis of the magnetic field of a (sometimes superconducting) solenoid. External injection using an appropriately shaped cathode and acceleration electrodes together with the focusing properties of the end fields of the solenoid guarantee an electron beam with a small diameter and a high density travelling on the axis. Typical parameters for this beam are an energy of several keV, a current of some amperes and a current density of the order of kA/cm^2. At the end of the solenoid the electron beam is blown up in diameter, owing to the fringe field, and dumped on a collector. Partial energy recovery is possible by applying a negative bias.

Ions are generated, for example, from the rest gas by collisions with the electrons. The thus-produced ions will stay within the space-charge potential well of the electron beam. If they are contained there for a long enough time successive ionization will take place up to a maximum determined by the ionization energy of the ion.

For the ECR source (invented and developed mainly at CEN Grenoble) a bottle-like magnetic field configuration (minimum B-field) is used, which assures the confinement of the plasma along the principal axis of the source, together with a multipole field that provides the radial stability. RF power is fed into this area from an external generator.

The solenoids can be air coils or they can be surrounded by iron. In the latter case a substantial gain in electrical power and also in the volume can be achieved.

For the production of the multiply charged ions, injection of gas (or evaporated solid or liquid materials) or injection of low-charge-state ions can be used. Inside the plasma chamber exists a region where the condition for the electron cyclotron resonance holds. In that region fast electrons are produced which ionize by successive collisions either neutral atoms or previously produced ions. Depending on the source parameters, electron energies of up to several hundred keV can be obtained. As the performance improves with increased RF frequency (and hence increased magnetic field), sources which use superconducting coils and frequencies around 30 GHz (using gyratron tubes) are being developed.

For the ECR source there are two important parameters. The first is the plasma frequency ω_p [in SI and Gaussian CGS units, respectively, in Eqs. (1) to (3)]

$$\omega_p^2 = \frac{e^2}{\varepsilon_o m_e} n_e = \frac{4\pi e^2}{m_e} n_e \ , \tag{1}$$

where e is the charge, n_e the density, and m_e the mass of the electrons; the second is the electron cyclotron resonance frequency in a magnetic field B:

$$\omega_c = \epsilon B/m_e \epsilon H/m_e c = 1.76 \times 10^{11} (B/\text{tesla})\ \text{s}^{-1} = 1.76 \times 10^{7} (H/\text{gauss})\ \text{s}^{-1} \ . \tag{2}$$

The energy of the electromagnetic waves with frequency ω must be able to enter the plasma, i.e. their frequency has to be higher than the plasma frequency ω_p. With increasing electron density in the plasma the plasma frequency increases. The density for which ω_p is equal to ω_c is called critical density:

$$n_c = \epsilon_o B^2/m_e = H^2/4\pi c^2 m_e = 9.71 \times 10^{18} (B/\text{tesla})^2\ \text{m}^{-3} = 9.71 \times 10^{4} (H/\text{gauss})^2\ \text{cm}^{-3} \tag{3}$$

Therefore to achieve better performance with higher electron densities requires higher magnetic fields and hence higher frequencies.

Originally gases were used to produce the ions. Ion production from solid materials can be achieved by evaporation of the solid material inside an electrically heated oven or by evaporation generated by the heat of the plasma.

Electron injection from either a normal gun or from some surface heated by the plasma with modest energies can greatly enhance the performance of the source. These developments were prompted by the discovery of the 'silicon effect'[12]. It was found that coating of the plasma chamber with a thin layer of SiO_2 resulted in better stability and higher charge states. This coating was produced by running the source with a mixture of SiH_4 and O_2. The disadvantage of this coating is, of course, its limited lifetime.

Other active electron emitters seem to be preferable. Spectacular enhancements of source performance are reported (Zunqui et al.[12]). As usual in this domain, the exact theoretical explanation is not straightforward, especially because it is very difficult to measure all the relevant plasma parameters.

A very interesting possibility of increasing the intensities has been found with the so-called 'afterglow' mode of operation[13]. In several sources it has been observed that switching off the μ-wave power results in a deconfinement of the ions. The result of this is an increase not only in the extracted current but also in the average charge state. The exact conditions for this mode are not yet very well known. The pulse length, and also the reproducibility, depend strongly on source construction and also on the additional injection of cold electrons.

3. The Lead Ion Source for the CERN SPS

In the past the CERN machines were mainly used to accelerate protons, electrons, and their anti-particles. Deuterons and alpha particles were studied only occasionally in machine tests. The interest in ion physics grew, however, and resulted in several special runs with deuterons and alpha particles in the Intersecting Storage Rings (ISR). The demand for heavier ions prompted runs with the Super Proton Synchrotron (SPS) using oxygen and sulfur ions[3]. As the ever-growing user community requested even heavier masses, a study was undertaken to provide a lead ion injector for the CERN accelerator complex[3]. Lead, in this context, stands, of course, for any heavy ions, e.g. for gold, bismuth, or possibly even for uranium, and certainly does not exclude the acceleration of lighter ions. Significant changes to the existing machines are necessary to provide CERN with the possibility of accelerating lead ions.

An ion source for fully stripped lead ions for the SPS requires essentially a whole chain of accelerators: the source of partially stripped ions, the linear accelerator, the booster synchrotron, and the PS (a 'proton' synchrotron). This type of 'source' works hence with accelerated ions which pass at high energy through a target of stationary electrons (i.e. a stripper foil).

3.1. Limits and Problems of the Existing Machines

All ions, independent of their charge-to-mass ratio, are subject to electric and magnetic forces and can hence be accelerated—at least in principle—in conventional accelerators. A lower charge-to-mass ratio, however, requires either higher fields or longer accelerators and acceleration times. This is the reason why high charge states are preferred, even if the resulting intensity is somewhat lower. So far no major upgrading of the existing CERN facilities had been carried out and therefore the linear accelerator already severely limited the selection of possible ions that could be accelerated. Departing from the usual charge-to-mass ratio of one, as in the case of protons, to 0.5, as for deuterons or alpha particles, would have required two times higher fields in the linear accelerator. Owing to the technology of the machine this would have been impossible. The way out was acceleration with half the proton velocity (the so-called 2 $\beta\lambda$ mode), requiring only lower, and technically feasible field levels roughly corresponding to the fields needed for proton acceleration. In the past, i.e. for the production of

deuterons and alpha particles, the usual duoplasmatron was quite adequate, provided it was fed with deuterium or helium. However, already the He^{2+} intensity was quite low and actually stripping of a He^{1+} beam after first acceleration was preferred.

During the more recent acceleration of oxygen and sulfur ions the charge states selected were O^{6+} and S^{12+}. To achieve these, a special ion source and more upgrading, mainly of the Linac, became necessary. A collaboration between GSI, Darmstadt, Germany, LBL, Berkeley, USA, and CERN took care of the necessary modifications.

Ion acceleration is a compromise between the efforts spent on the ion source, on the one hand, and on the accelerator, on the other hand. A simple ion source (e.g. duoplasmatron, Fig. 1 [1]), gives a low charge state and requires a long linear accelerator. A more complicated ion source (EBIS, ECR source, or a laser ion source) can yield very high charge states and requires only a short accelerator (see, for example, Fig. 5 in subsection 4.1, where a CO_2 laser of fairly high power produced Au^{51+} directly from the target in 1983). An economical solution will, in general, aim for reasonably high charge states.

For all ions, even the fully stripped ones, the charge-to-mass ratio is smaller than for protons; acceleration and focusing is therefore more difficult. If identical acceleration rates and particle trajectories are desired, the electrical accelerating fields and the magnetic focusing fields must be increased in such a way as to keep constant the product of field times charge-to-mass ratio. As magnetic and electric fields have technical limits, it is, in general, impossible to use an accelerator, which is well designed for protons, for the acceleration of heavy ions. Special designs are needed to cope with the low charge-to-mass ratio and the low acceleration rate. This requires not only long linear accelerators, but also long acceleration times in the circular machines, resulting finally in lower energies (at least if measured in energy per nucleon).

For the linear accelerator different structures can be envisaged, such as for example a 2 $\beta\lambda$ Alvarez structure[14], a $\beta\lambda/2\beta\lambda$ hybrid Alvarez structure (Warner et al.[15]), or an interdigital H-structure (Ratzinger et al.[15]). The circular machines can be used with some modifications, needed because of the low velocity of the ions.

3.2. Intensity Losses

There are different reasons for intensity losses in proton accelerators, such as mismatch between acceptance of a machine and emittance of the beam coming from the upstream machine, space-charge effects at higher intensities, and different sorts of instabilities. All these loss mechanisms are, of course, also relevant for heavy ions. Additional losses occur for the latter owing to the capture or loss of electrons by interaction with a residual gas. Both effects change the charge-to-mass ratio and result in immediate loss of the particle concerned in a synchrotron, and will spoil the beam quality in a linear accelerator. In general, loss of electrons is dominant at high energies and recombination is important at low energies, the transition between these two regimes depending on the ionization energy of the ion.

To evaluate the importance of the effect, the cross-sections for charge-exchange reactions must be known. Their values depend on the ion, on its charge state, on its velocity, and on the residual gas. In the range of interest there are lots of theoretical calculations, but only very few experimental data—mainly from GSI and LBL. Empirical formulae have been developed in both laboratories for interpolation and extrapolation of the measurements.

3.3. The Plans at CERN[16]

As in the past for the oxygen and sulfur ions, an international collaboration with laboratories in France, Germany, India, and Italy will contribute to the development of the lead ion source.

There are several parameters which have to be optimized:

- the charge state coming from the ion source,
- the energy of the linear accelerator,
- the energy at which intermediate and final stripping will be performed,
- the required, or tolerable, vacuum pressure in the circular accelerators,
- the desired energy at the exit of the circular accelerators.

Several iterations were required to optimize the performance and to minimize costs. The final layout is presented in Fig. 3a.

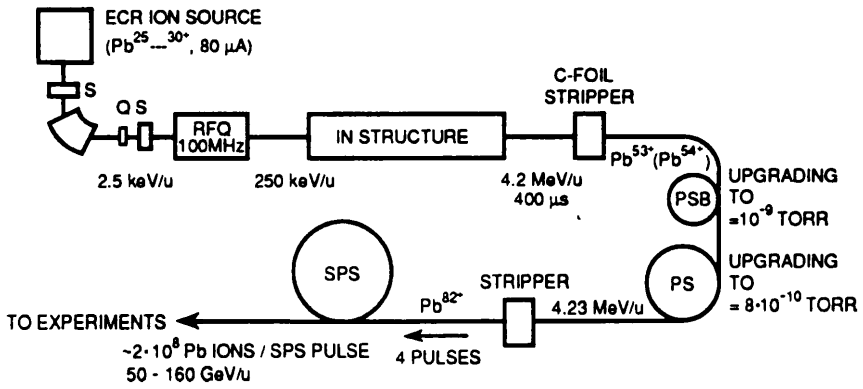

Fig. 3a Schematic layout of the lead ion accelerator complex[16]

The ECR source that will be used is based on the existing state of the art. It will provide 80 μA (electrical) of lead ions with a charge state of 28+. With the proposed scenario this performance should provide more than the intensity of 5×10^7 ions per SPS pulse required by the experiments.

The choice of this source with its high charge state allows minimization of the cost of the linear accelerator, still providing the required intensity. Higher charge states could also possibly be achieved, with other sources, but would unfortunately drastically reduce the intensity. Lower charge states are feasible and would yield higher intensities. However, this would lengthen the linear accelerator part and hence increase the cost.

In addition, more intermediate stripping could become necessary, again reducing the increased intensity by almost one order of magnitude per stripper.

3.3.1. Low-Energy Acceleration

The energy of the ions at the exit of the ion source is of the order of 2.5 keV/u. For further acceleration of the slowly moving ions a radio-frequency quadrupole (RFQ) with its electric focusing is nowadays the obvious choice. As in all RF accelerators the transverse focusing is weakened by a defocusing effect, which is a consequence of the phase stable acceleration. This defocusing is inverse to the beam energy and hence most unfavourable at the low-energy end of the Linac. To counterbalance this effect, operation at a lower frequency (101.28 MHz) has been chosen, where the focusing in terms of betatron phase advance per period is more efficient.

The choice of this frequency allows the peak surface fields to be kept below twice the Kilpatrick limit.

In this frequency range a 4-rod RFQ will be the best solution. Beam matching into the RFQ will be performed with magnetic solenoids.

3.3.2. The Linac

For further acceleration of the ions an interdigital H-structure has been chosen. This structure has been developed and used at Munich and other places. GSI has built an accelerator using this structure to accelerate ions of a similar energy range and with a charge-to-mass ratio close to the CERN requirements[16]. The advantages of this structure are its compact size, its low RF power consumption (due to a high shunt impedance), and its high accelerating rate. The disadvantages are the difficulties in calculating the structure and the delicate RF tuning to achieve the desired field distribution. This structure also needs a better precision of RF levels and phases. Whereas GSI requires an output energy of 1.4 MeV/u, the CERN scheme calls for an energy of 4.2 MeV/u, requiring three accelerating structures as compared to that of GSI.

The first tank, similar to the one developed at GSI, will run at the same frequency as the RFQ, whereas the two subsequent tanks will operate at twice the frequency. This substantially reduces the length of the accelerator.

At this stage it should be mentioned that the selected output energy of 4.2 MeV/u stems from a careful optimization and several reiterations. As the subsequent machines need at least one intermediate stripping to reach sufficiently high energies, and because any intermediate stripping provokes drastic intensity losses, only one place has been selected for intermediate stripping: the exit of the Linac. The energy there determines the charge state for the subsequent machines and hence the necessary vacuum conditions (Fig. 2), the particle velocities, and the required upgrading of pulsed elements.

3.3.3. Acceleration in the Synchrotrons and Booster

Beam transport lines, and injection and ejection elements will, in general, need upgrading to cope with different magnetic rigidities and pulse lengths. The vacuum requirements can be estimated from the graph presented in Fig. 3b.

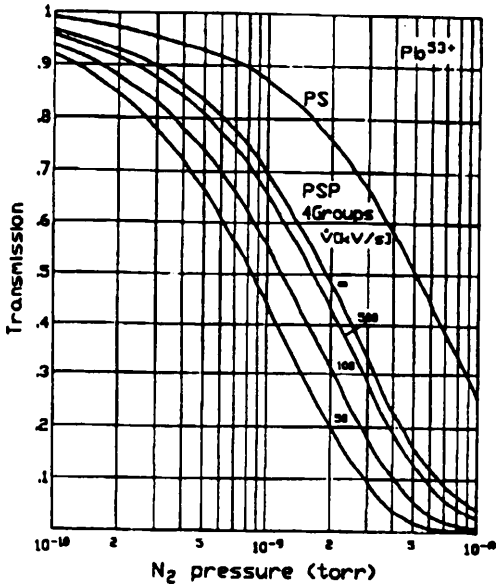

Fig. 3b Recent results of transmission of Pb^{53+} in the PSB and the PS [3,16]

The maximum frequency swing (2.95–8.05 MHz) of the Proton Synchrotron Booster (PSB) accelerating cavities is not sufficient to cope with the variation of the relativistic β-factor of the lead ions. Therefore, a change of the harmonic number is required from 17 to 10, involving debunching and adiabatic recapture on an intermediate flat top of the magnet cycle. However, the main modification this machine will need is the improvement of the vacuum from the 1 to 2×10^{-8} mbar at present to about 1×10^{-9} mbar. This will be accomplished by the installation of 45 titanium sublimation pumps, the changing of turbo pumps, prebaking, and general cleaning. To achieve a better safety margin and/or a shorter pump-down time, changes and modifications of kickers and septa may be required so that they can be baked *in situ*.

3.3.4. Proton Synchrotron

Lead ions in the Proton Synchrotron (PS) will be interleaved with other particles such as protons, antiprotons, electrons, and positrons. The transport line between the PSB and the PS cannot be changed from one pulse to the next. This imposes that the PSB to PS ion transfer has to take place at the same magnetic rigidity (5.634 T·m) as the standard 1 GeV proton transfer. The 40 bunches from the PSB will be captured by 20 buckets using the standard ferrite-tuned RF cavities in the PS ring.

No transition crossing will be required. Extraction from the PS will be carried out as a standard single-turn fast extraction. A stripping foil will be located in the transfer line PS–SPS.

A substantial improvement of the vacuum is also needed in the PS. To achieve an average pressure of around 10^{-9} mbar about 150 titanium sublimation pumps will be installed. As in the case of the Booster, additional upgrading may be necessary if pumping-down times are too long.

3.4. Future Improvements

The present planning will satisfy (at least for the time being) the proposed fixed-target experiments. Higher intensities may be interesting in the future, especially in the case of colliding beams. The LHC in the LEP tunnel is certainly the ultimate scenario that can be envisaged in the near future, where energies of about 3 TeV/u per beam could be reached[2].

For an optimum luminosity in this machine, intensity increases become necessary. They can probably be achieved in several ways. A straightforward possibility is 'funnelling'. In this scheme a second ion source and a second RFQ (also running at 100 MHz) would be used to fill the empty buckets of the 200 MHz Linac. Joining the two beams from the two RFQs would be performed by a 200 MHz deflector.

Another possibility for higher intensities is the simultaneous acceleration of several charge states coming from the ECR ion source. After the stripper there will be no difference between the various ions, provided proper care is taken regarding the position of the bunches in the longitudinal phase space.

At CERN there are several machines that could be used for storage and cooling. Storage schemes making use of the d.c. beam coming from the ECR source could drastically enhance the intensity in our accelerators. One possibility in this context could be injection into the Low-Energy Antiproton Ring (LEAR), or a similar storage ring, and to apply cooling in transverse phase space.

The greatest hopes for intensity increases are of course linked to progress in the ion source field.

It should be mentioned that the development of the ion sources for heavy-ion accelerators will have an enormous technological application to the production of submicron microelectronics of very high quality and high accuracy[17], the applications of which are elaborated in more detail in the article by K. Bethge in this book.

4. Phenomena of the laser ion source

One of the very first experiments after the discovery of the laser was the irradiation of solid targets in vacuum and the observation of the generated plasma and its expansion into vacuum. The emission of electrons and ions was measured from the time of flight of these charges when arriving at a probe connected to an oscilloscope. The very early measurements with the irregularly spiking ruby lasers of a maximum power of up to some 100 kW showed ion energies in the range of a few to 10 eV, corresponding to the thermal expansion of the generated plasma whose temperature was about 20,000 to 40,000 K (corresponding to 2 to 4 eV) [18]. This fully thermal behaviour of the laser-produced plasma is typical for laser irradiation with powers less than 1 MW and is a most extensive field of the technological applications of lasers for welding, cutting,

surface hardening of steel, and many other techniques as elaborated, for example, in the book by Ready[18].

The change to laser powers above 1 MW indicated basically non-thermal phenomena, with the sudden appearance of ion energies of several keV, and a number of 10^{15} or more highly charged ions are produced by the laser pulses in the range of 10 ns duration[19]. We shall discuss these anomalous and typically non-linear effects in detail in subsection 4.1 in order to provide a practically complete overview and arguments on the advantages as well as the disadvantages of using this ion emission as a source for accelerators.

4.1. General Overview

Firstly, we shall present in this subsection, an overview of observed phenomena of ion production by lasers for an ion source. A typical measurement of ion energies from the time of flight is shown in Fig. 4a [20]. A CO_2 laser of varying intensity $I = \phi$ in W/cm^2 is shown, where at the lowest intensity of 10^{12} W/cm^2, a first narrow peak can be recognized which corresponds to the photoemission of electrons from the probe due to the UV photons of the laser-produced plasma. This is an ideal mark for the time zero (neglecting the speed of light for the photons between the target and the probe). The signal that follows later corresponds to the ions of the more or less thermalized, expanding plasma. At higher intensities there are maxima appearing in the ion signal corresponding to very high ion energies much above the thermal properties. Energetic ions of this type have been observed since the first multi-kiloelectronvolt ions were detected by Linlor[19] with ruby laser powers only of several megawatts, and always at these higher laser powers, in numerous experiments around the world.

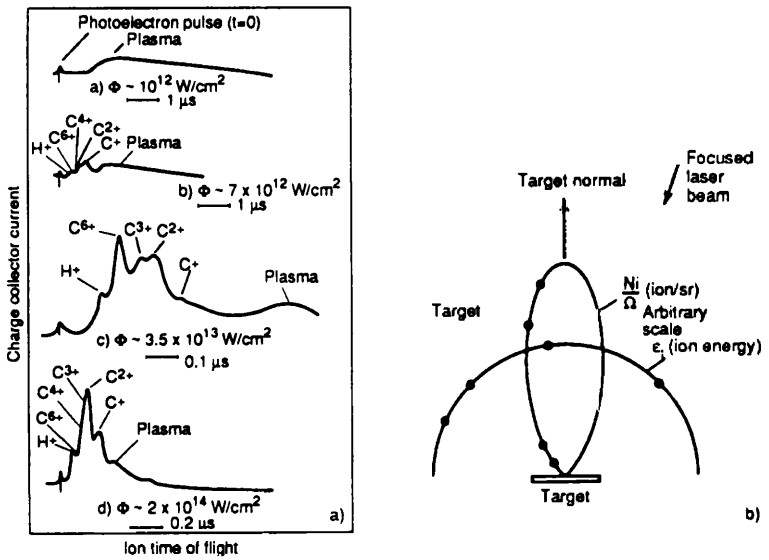

Fig. 4 Ion emission of up to 2 MeV energy from carbon-dioxide laser irradiated carbon and aluminium[20]. a) Oscilloscope signals for various laser intensities and b) angular distribution

Use of differentiating diagnostics with Thomson parabolas and other electrostatic or magnetostatic analysers confirmed that there were truly highly charged ions observed, for example[20], Al^{13+}, or much higher ionization states from other elements, for example[21] Co^{27+}. The energetic ions could contain 80% of the whole ion energy[20] and show a strong directivity perpendicular to the target (Fig. 4b). In this case, 2.7×10^{14} ions were counted as being energetic ions whose energy was between 200 keV for singly charged aluminium linearly increasing in dependence on the charge number to $Z = 11$, where the ion energy was about 2 MeV. Apart from the very fast megaelectronvolt ions and the low energetic thermal ions there was a third group of plasma detected between two groups[20]. The additional diagnostics permitted a differentiation of the aluminium ions of the higher charge numbers of the target from precursing hydrogen ions or carbon and hydrocarbon ions owing to the contamination by the oil from the vacuum pumps. The explicit clarification of megaelectronvolt ions was reported from tungsten targets[22]. The fact that these ions could not only be diagnosed by time-of-flight measurement, but really got their high megaelectronvolt energy from the spot of their origin within the target at the area of laser interaction, could be confirmed by Rode[23], who measured the X-ray spectra of phosphorous ions in the range of a few ångström, and saw, for example, the Doppler shift of P^{13+} ions of 2 MeV by irradiation intensities of 2×10^{15} W/cm^2 of a neodymium glass laser.

Using the HELIOS CO_2 laser, Au^{51+} with maximum ion energies of 310 MeV were measured (see Fig. 5, which is a copy of an overhead projection[24,25] since this fact was not published elsewhere), whilst experimental results were related to ion energies per nucleon (see subsection 5.2, especially Fig. 13) from which energies of gold ions of up to 500 MeV can be confirmed[25]. For an extension of the measurements from the HELIOS to the very large ANTARES laser, a very sophisticated numerical evaluation[26] resulted in the prediction of ion energies up to 5 GeV.

SUMMARY (CONT'D)

IN THE 'HEATED' DISC TARGET PLASMA,

- A = 181, Z = 51 IONS ARE THE DOMINANT PLASMA
- MAXIMUM KINETIC ENERGY = 310 MeV
- AVERAGE GLOBAL PLASMA MOTION ORGANIZES ITSELF TO GIVE THREE ELECTRON TEMPERATURES

IN THE 'COLD' SPHERICAL TARGET PLASMA,

- PROTONS ARE THE DOMINANT PLASMA. PROTON CURRENT DENSITY IS A FACTOR OF 100 GREATER THAN HEAVY ION COMPONENT
- MAXIMUM KINETIC ENERGY = 2 MeV
- AVERAGE GLOBAL PLASMA MOTION ORGANIZES TO GIVE TWO ELECTRON TEMPERATURES

Fig. 5 Reproduction of the reported measurement of laser-produced 310 MeV Au^{51+} ions[25]

These facts alone were most impressive when considering the laser ion source as a candidate for use in accelerators. Numerous other problems, however, had and still have to be clarified beforehand. There is the question of the thermal width of the highly charged energetic ions and how this can be solved by accelerator techniques; there is also the problem of the extraction of the ions after their generation for the subsequent pre-acceleration by injection into a linac, or quadrupole accelerator, or a cyclotron, and many more questions[27].

4.2. Developments of an Ion source for Injection by a Linac

One further point of importance is the technology of the lasers and the engineering of the target for a very large number of high repetition rates and fully reliable functioning of the laser ion source. These developments have succeeded, for example, at 1 Hz operation for more than one million pulses[28] or for filling 4000 shots of 1 Hz of magnesium ions into an accelerator, in finally each producing pulses of 10^9 C^{5+} or of 10^8 Mg^{12+} or of 5×10^{10} C^{4+} in a proton synchrotron with energies of 2 GeV/u after injection through a linac[29]. We shall report on these technological developments in the following paragraphs of this subsection, whilst the physics is discussed in detail in Section 5.

Research and development on the laser ion source have been pioneered since about 1969 by Prof. Yu.A. Bykhovski of the Engineering Physics Institute in Moscow, whose work has also been followed up by his co-workers in other institutes, such as the JINR, Dubna, or the ITEF in Moscow. The problems involved are still rather complex, since a number of anomalous processes known from laser fusion research are involved; these refer to the properties of the recombination of ions, even the appearance of negative ions, whilst the main studies are the usual detection of highly ionized heavy ions, their angular distribution and interaction with magnetic fields, their bending and selection by fields, and the injection into accelerators.

Whilst the thermal and rather anomalous non-linear properties of the ions from laser-produced plasmas were studied intensively in scientific laboratories around the world, the application for ion sources in accelerators was first discussed in the Western countries by Peacock and Pease at the Culham Laboratory[30] before 1968 and in patents. Later work[31] was strongly supported by the results achieved after many years by the above-mentioned Moscow Institute.

Some unique results of the Munich ion source (Korschinek et al.[31]) will be discussed, especially under the physics problems in Section 5.

The work with the classical proton synchrotron at Dubna, mostly favoured by N.G. Flerov, is the longest known activity for filling accelerators with laser-produced plasmas. Monchinski[29] now uses transversely excited atmospheric pressure (TEA) carbon-dioxide lasers. He used neodymium glass lasers in the seventies, but did not find them very useful—at least at the low energies and high repetition rates available up to about 1980. Monchinski's carbon-dioxide laser has a typical 100 ns first pulse and a subsequent long pulse of about equal energy of 1 to 2 μs length. The laser has been modified in such a way that the long pulse can be switched off within the laser cavity

(obviously a rather new modification). The target chamber which can be used with most uncomfortable solid targets, including magnesium, contains a cylindrical target which can be rotated step by step for each shot. Liquid metals at the same spot as the target are under experimentation. With the present cylindrical rotating target, 4000 shots of 1 Hz sequence in each run have been performed without opening the chamber. The salt entrance lens of the laser beam was protected against the emitted ions by a plastic foil which was designed so that it could be removed from the front of the lens and renewed automatically after a number of shots.

The ion beam is injected through a tube about 3 m in length to an ion-bending system, turning the beam about 35° and selecting the ions of desired ionization into the axis of a following linac. After this the ions are guided into Dubna's first proton synchrotron. The linac is for 20 MeV protons and for 5 MeV/u ions. An e/m ratio of 1/3 is the limit before breakdown occurs.

The carbon-dioxide laser produces a first pulse of 7 J total energy, with 30 MW and 100 ns duration. The following long pulse tail is cut off. This was considered necessary for high fluxes for higher charged ions; otherwise the long pulse could be used. For the synchrotron, 20 μs long pulses of C^{4+} have been produced resulting in 5×10^{10} C^{4+} ions with an energy of 4 GeV/u in the synchrotron. Up to 10^9 C^{5+} and 10^8 Mg^{12+} ions were produced without the laser pulse tail and consisted of 5 μs pulses.

4.3. Laser Ion Source using Cyclotrons

An alternative method of generating the ions from a laser-produced plasma for injection into a linac is to generate the ions at the central axis of a cyclotron. This is being studied, especially for the source of heavy ions in a project at Dubna under the direction of Yu.Z. Oganesian. The existing 2 m or 4 m cyclotrons are used as described below. Moderate- and high-repetition-rate laser pulses have produced up to 10^{10} ions of C^{3+} or ten times less Si^{7+} ions in the synchrotrons into which the ions were injected after leaving the cyclotron. This was reported by Kutner, Bykovsky et al.[32] who referred to earlier work[33].

A 10 J carbon-dioxide laser pulse of 60 ns duration produces 18 times ionized niobium with a laser intensity of 3×10^{10} W/cm^2. The ions are being produced in a tube (Fig. 6) in the central axis of the cyclotron of 2 or 4 m diameter with a laser irradiation from above. The cyclotron magnetic field B is also acting inside the tube so that the plasma generated from the target (Fig. 6) expands as a slim plume within the tube. When passing the grids of high voltages, ions of desired specifications are extracted into the cyclotron and subsequently accelerated. After the cyclotron, the ions are injected into a linac, reaching an energy of 10 MeV/u before going to the synchrotron. Including a mechanism with an 'exotic beam' for charge exchange, they achieved the above-mentioned pulses of C^{3+} ions of 10^{10} and ten times less ions in Si^{7+} pulses. However, the pulses after the 2 m cyclotron are very long, of 5 μs duration. Ten times shorter pulses are needed to better fit the circumference of the following synchrotron.

The configuration is ideal for the cyclotron since its magnetic field is simultaneously used for the guiding of the plasma plume. The scheme has been studied with small laser pulses of 1.5 J energy only, with 10^{10} W/cm^2 intensity, where Fe^{+12} ions have been produced.

It was also possible to work with neodymium glass laser pulses as low as 50 mJ and 2×10^9 W/cm^2 intensity to achieve C^{+3} with 1.5×10^{10} ions per pulse. Since there was an instability of the plasma observed in the magnetic field parallel to the plume, a metallic cylinder was introduced around the plasma plume which fully stabilized the plasma.

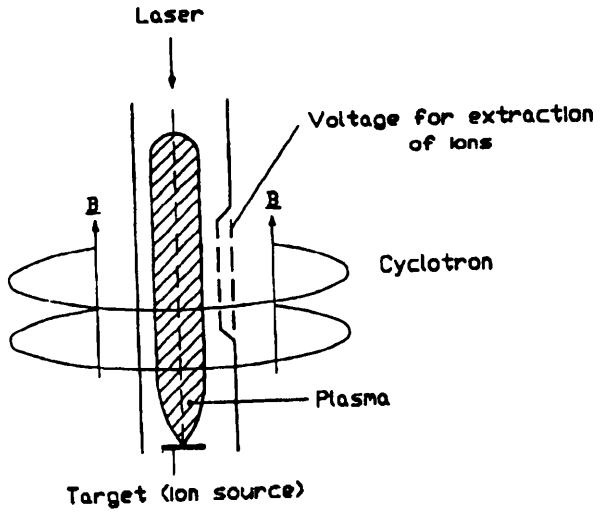

Fig. 6 Laser ion source in the axis of a cyclotron with an extraction voltage[31]

Further tests were performed to see what happens if the magnetic field is not parallel to the plasma plume, as in Fig. 6, but perpendicular to it. In this case the target was in front of the electrostatic grid for the extraction of the ions into the cyclotron. The laser had to be obliquely incident at 45°. Carbon-dioxide laser pulses of 10 J, 60 ns duration and 3×10^{10} W/cm^2 intensity were used. Once again Nb^{18+} was observed, but the ion distribution showed a butterfly-wing profile. This was due to the charge separation by the magnetic field, and a further action of the magnetohydrodynamically-generated electric field was expected. The details of the mechanisms are not yet understood. It was suggested that the $E \times B$ drift of plasma has to be included to describe the plasma motion. The result is that 1000 times more ions for 14 times ionized Ta have been observed.

Most of these experiments concerning technological developments of laser ion sources used only medium-size or even smaller lasers, where the main properties of the ions in the usual cases were of thermal nature; they did not have the suprathermal properties of the above-mentioned energetic ions. We shall come back to this question after reporting on the known general physical problems of laser interaction with plasma in Section 5.

5. Physics of Laser Ion Sources

As mentioned in the preceding section, the laser interaction with solid targets in vacuum generates plasma with a complex property of the emitted ions. These phenomena can be advantageous or may cause difficulties for the laser ion sources. This is the reason that we are presenting a short review of the physics of the phenomena involved. This was summarized in several reviews[34-36] and monographs[37-42], where the main interest of the applications was not so much the laser ion source but the use of the lasers for igniting exothermal thermonuclear fusion reactions.

This broad field of research indicated in much detail how the complexity and difficulty of the interaction mechanism are due to non-linearities of the hydromechanical properties of the generated plasma (non-linear forces) and the non-linearity of the optical constants when these depend on the laser intensity (see subsection 5.1). One phenomenon observed was the generation of suprathermal 'hot' electrons and resonances (subsection 5.2). Another result is the mechanism of self focusing and filamentation (subsection 5.3), whilst the mechanism of parametric instabilities was a topic of very intensive studies (subsection 5.4).

In order to analyse the non-linear forces of laser-plasma interactions, the properties of the highly inhomogeneous plasmas, which caused the internal electric fields and double layers in plasmas, had to be studied. The earlier known ambipolar fields were a special case only of a very much more general oscillating phenomenon with consequences of surface tension contrary to any earlier expectation (subsection 5.5). The most complex property of laser-plasma interaction was understood within the very last few years only by the experimental confirmation of a very irregular temporal pulsation, or stuttering in the range of 10 to 40 ps duration (subsection 5.6). Some intuitively introduced optical methods for the smoothing of the interaction appeared to be very successful in overcoming this pulsation problem, though the reason for which these smoothing methods were introduced was motivated by the need to solve a different problem.

Only now, after 30 years of laser-plasma interaction studies, covering most advanced diagnostics and experimental techniques with resolutions in the range down to picoseconds or less and micrometres[40,41], may a solution have been found for the physical understanding of direct drive[39,42] laser interactions with plasmas for fusion. We also know now what physics phenomena will be covered for the development of the laser ion source. In fact, the study of the laser ion source[31] produced, in a very independent and unintentional way, results which confirm the very recent view of the physics solution of the laser-plasma interaction as will be discussed in subsection 5.6.

5.1. Non-linearities in Hydromechanics and Optical Response

As mentioned concerning the phenomena of the laser ion source, the surprising and confusing results of laser interaction with plasmas appeared simply from the study of the ion energies from laser-produced plasmas. When the laser power was less than about 1 MW, the generated plasma behaved absolutely classically, with temperatures of a few 10 thousand degrees (a few electronvolts)[17]. The electron emission was also fully

classical[43], with emission current densities of about 100 mA/cm^2, exactly as limited by the Langmuir–Child space-charge law. However, when applying laser pulses of higher than 1 MW power, a basic change appeared[44]: the electron current densities—contrary to what was expected from the mentioned space-charge limitations—arrived at 10 to 100 A/cm^2 [44].

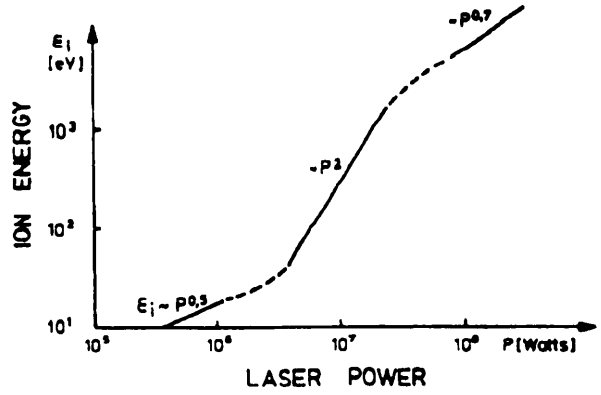

Fig. 7 Maximum ion energy of thermal properties below about 1 MW laser irradiation and superlinear increase to keV ions above MeV with some saturation at higher laser powers[38,39]

The ions whose maximum energies suddenly changed from a few electronvolts for laser powers below megawatt to kilo-electronvolt above megawatt[19] had a clearly superlinear, nearly quadratic increase on the laser power (Fig. 1.1 of Ref. 39)[45] which, however, for higher laser powers arrived at some saturation with an exponent of less than one at higher powers (Fig. 7) [38,39]. These non-linear fast ions flying preferentially against the laser light with energies of several kilo-electronvolts, could be seen directly from image converter pictures[46], Fig. 8. On ruby laser irradiation with 2 to 10 J pulses of 10 to 20 ns duration on spherical aluminium of a few 100 μm diameter in the laser focus, a central spherical plasma was produced which fully followed a gas dynamical expansion with temperature between 10 and 70 eV [46], exactly as predicted numerically from the Zeldovich–Reiser Model as used by Basov and Krokhin[47] and Dawson[48], and which was improved by taking into account the temporal increase of the radius during the interaction (see Ref. 39, Fig. 5.1).

The outer part of the plasma with maximum ion energies up to 10 keV moving asymmetrically towards the laser, showed a typically non-linear behaviour where the maximum ion energies increased with an exponent of nearly 1.5 over the laser intensity. Under the conditions of this experiment, the amount of energy being transferred to the non-linear part of the plasma was about 5%, whilst the thermal plasma consumed nearly 95% of the interacting laser energy. This should be mentioned in view of the experimental result that under conditions of much higher laser intensities (the equivalent intensity of CO_2 lasers comparable with that of ruby lasers is to be converted by a factor of 210 because of the $I\lambda^2$ law[38,39] for intensity I and wavelength λ) as shown in

Fig. 4, 90% of the interacting laser energy went into the fast ions of more than 100 keV energy[20]

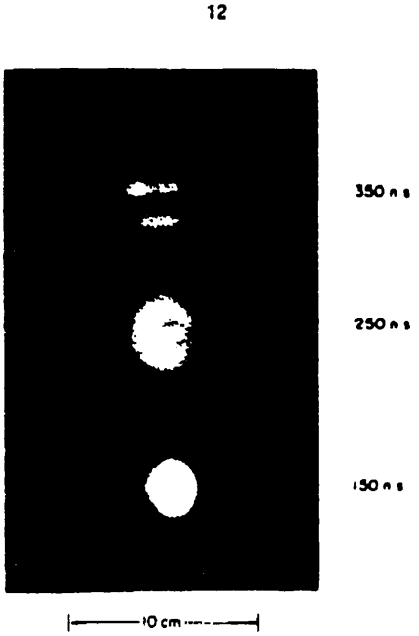

Fig. 8 Side-on framing camera pictures of laser-irradiated aluminium spheres (from the left-hand side) showing the central thermal plasma of some 10 eV temperature and the asymmetric (half-moon like) keV ions moving with preference against the laser light[39,46]

There was an initial discussion as to whether the kiloelectronvolt ions generated in the plasmas, whose temperatures were only some electronvolts, are produced in the electric field of the plasma surface. The light electrons at this temperature leave the plasma with high velocities, leaving behind the heavy ions and generating an electric field corresponding to a double layer (see subsection 5.5). If an ion is speeded up by this ambipolar electric field to the electron velocity, kiloelectronvolt energies are immediately produced. The problem is, however, that this double layer has the thickness of a Debye length; therefore only about 10^9 or less ions can be accelerated in this way. This has been shown experimentally for a group of fast ions from a laser-produced plasma of about this number where no dependence on the polarization of the light has been detected[49].

Since the number of the ions of kiloelectronvolt energy was 10^{14} and more from the beginning[19] and was reproduced continuously in all other known experiments[39], the electrostatic mechanism for the acceleration could not be applied, at least not for the main part of the kiloelectronvolt ions. This was the motivation to look for non-linear hydrodynamical processes of the laser interaction with plasma. The first result was[50] that forces of direct electrodynamic interaction without heating the plasma dominate any gas-dynamic force density (the negative gradient of the gas-dynamic pressure P) if the laser intensity is sufficiently high, i.e. higher than 10^{14} W/cm^2 for neodymium glass lasers, and 100 times less for carbon-dioxide lasers (with respect to the $I\lambda^2$ law[38]). The

essential reason for the force was that the gradient of the plasma density as expressed by the complex dielectric constant $\tilde{n}$ was determining the force which was called a 'non-linear force'. For perpendicular incidence of the laser wave on a striated plasma, the force was[50]

$$\mathbf{f}_{\mathrm{NL}} = -(1 - |\tilde{n}|^2)\frac{\mathbf{E}^2}{16\pi}\frac{\partial}{\partial x}\frac{1}{|\tilde{n}|} \,. \tag{4}$$

The refractive index $\tilde{n}$ is given by

$$\tilde{n}^2 = 1 - \frac{\omega_{\mathrm{p}}^2}{\omega^2(1 - i\nu/\omega)} \,, \tag{5}$$

where ω is the laser radian frequency, ω_{p} is the plasma frequency given by

$$\omega_{\mathrm{p}}^2 = \frac{4\pi e^2}{m_{\mathrm{e}}} n_{\mathrm{e}} \,, \tag{6}$$

e being the charge, m the mass, and n_{e} the density of the electrons in the plasma and

$$\nu = 8.51 \times 10^{-7} \frac{Z n_{\mathrm{e}}}{T^{3/2}} \ln[1.55 \times 10^{10}\, T^{1/2}/(Z n_{\mathrm{e}}^{1/2})] \tag{7}$$

being the collision frequency[38,39] of the electrons with ions in the plasma having a temperature T.

The time-averaged non-linear force density in the case of general geometry for nearly stationary (non-transient) incident laser pulses was shown to be[39,51]:

$$\mathbf{f}_{\mathrm{NL}} = \frac{1}{c}\mathbf{j} \times \mathbf{H} + \frac{1}{4\pi}\mathbf{E}\nabla \cdot \mathbf{E} + \frac{1}{4\pi}\nabla \cdot (\tilde{n}^2 - 1)\mathbf{E}\mathbf{E} \tag{8a}$$

$$\mathbf{f}_{\mathrm{NL}} = \nabla \cdot \left[\mathbf{T} + \frac{\tilde{n}^2 - 1}{4\pi}\mathbf{E}\mathbf{E}\right] - \frac{1}{4\pi c}\frac{\partial}{\partial t}\mathbf{E} \times \mathbf{H} \,, \tag{8b}$$

where $\mathbf{E}$ and $\mathbf{H}$ are the electric and magnetic laser field strengths, $\mathbf{j}$ is the current density in the plasma, and $\mathbf{T}$ is the Maxwellian stress tensor. The correctness of the formulation, and of this formulation (8a) only, was proved by the conservation of momentum. Any adding or substracting of non-trivial terms of Eq. (8a) results in an imbalance of the momentum. The tensor algebraic equivalence of Eq. (8b) derived from Eq. (8a) is the first *hydrodynamic* derivation of the Maxwellian stress tensor (instead of the historic *elastomechanic* derivation) and it occurred for the first time at the force density in the dispersive and dissipative case for plasma of any frequency whilst an earlier derivation of Eq. (8b) was for non-dispersive, non-dissipative dielectric fluids for moderate frequencies only, as shown by Landau and Lifshitz (see Refs. 38, 39, 51).

Equation (4) is the special geometric case resulting from Eqs. (8a) and (8b) and is formally identical with the ponderomotive force as known since 1846 as electrostriction in electrostatics. It is also identical in high-frequency fields with gradient in the average intensity, for example in standing waves or in stationary beams (see Weibel and Kibble

in Ref. 39). However, the result (4) showed for the first time the effect of the dielectic inhomogeneity of the laser-irradiated plasma. The suggestion[50] that the laser light causes a dielectric explosion was splendidly confirmed numerically by Shearer, Kidder and Zink[52] (Fig. 9). Whilst any gas-dynamic interaction will result in monotonous density profiles of the plasma, the non-linear force produced a density minumum (caviton) as a result of the dielectric explosion. This caviton has been measured by numerous authors[38,39] since 1975 as proof of the predominance of the non-linear force over the thermokinetic forces.

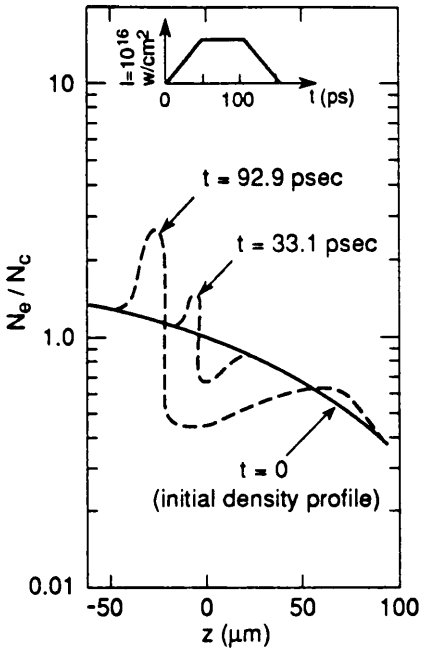

Fig. 9 Computations of a plasma density profile with an electron density N_e related to the critical density $N_c = 10^{21}$ cm^{-3} of neodymium glass lasers for a laser pulse as shown in the upper diagram incident from the right-hand side for various times t with the discovery of the density minima (cavitons) generated by the action of the non-linear force; from Shearer, Kidder and Zink[52]

For the case of fast time-dependent laser irradiation, a strong controversy appeared concerning the additional terms of Eqs. (8a) and (8b) where six different schools have six different formulations[53]. These formulations were still for approximative time dependences only and, by adding a further term, the closed formulation of the complete transient solution was derived[54]

$$\mathbf{f}_{\mathrm{NL}} = \frac{1}{c}\mathbf{j} \times \mathbf{H} + \frac{1}{4\pi}\mathbf{E}\nabla \cdot \mathbf{E} + \frac{1}{4\pi}\left(1 + \frac{1}{\omega}\frac{\partial}{\partial t}\right)\nabla \cdot \mathbf{E}\mathbf{E}(\check{n}^2 - 1) \tag{9a}$$

$$\mathbf{f}_{\mathrm{NL}} = \nabla \cdot \left[\mathbf{E}\mathbf{E} + \mathbf{H}\mathbf{H} - \frac{1}{2}(\mathbf{E}^2 + \mathbf{H}^2)\mathbf{1} + \left(1 + \frac{1}{\omega}\frac{\partial}{\partial t}\right)[\check{n}^2 - 1]\mathbf{E}\mathbf{E}\right]/4\pi - \frac{1}{4\pi c}\frac{\partial}{\partial t}\mathbf{E} \times \mathbf{H}\,, \tag{9b}$$

the general validity of which was proved by Lorentz and gauge invariance[55].

Whilst the general gas-dynamic and non-linear forces for a hydrodynamic model of laser-plasma interaction have been established in this way, another non-linearity to be discussed is the intensity dependence of the optical constants (5). The first modification appeared when the oscillation energy ϵ_{osc} of the electrons in the laser fields of an intensity I expressed here in relativistic form,

$$\epsilon_{osc} = m_o c^2[(1 + 3A(I)I/I_{rel})^{1/2} - 1] , \tag{10}$$

using a correction factor $A(I)$ monotonously growing from 1 for $I \ll I_{rel}$ with increasing intensity to 1.06 and using the relativistic threshold intensity I_{rel} (with the electron rest mass m_o and the vacuum velocity c of light)

$$I_{rel} = 3m_o^2\omega^2c^3/(8\pi e^2) . \tag{11}$$

The numerical value of Eq. (11) is

$$I_{rel} = 3 \times 10^{18}/\lambda^2 \quad \mathrm{W/cm^2} , \tag{12}$$

expressing the laser wavelength λ in micrometres. The relativistic threshold is that intensity where the oscillation energy of the electron in the laser field is $m_o c^2$ using the rest mass m_o of the electron.

For high laser intensities I, the electron mass in the optical constants (5) to (7) has to be relativistically corrected

$$m = m_o/(I - 3A(I)I/I_{rel})^{1/2} \tag{13}$$

and the electron energy is then not only given by a chaotic motion due to a temperature T in Eq. (7) but also by an effective temperature

$$T_{eff} = T + \epsilon_{osc}/2k \tag{14}$$

using the Boltzmann constant k.

For high intensities, the collision frequency (7) is then dependent on the intensity I with a power of -3/2 as initially derived quantum mechanically by S. Rand and later from plasma theory [see Eq. (6.59) of Refs. 38, 39]. The question of the change of this exponent to -1/2, because of the quantum modification of the Coulomb collisions[38] as an expression of the inclusion or neglect of stimulated emission in the ordinary inverse bremsstrahlung mechanisms, has been pointed out[39], but may be an effect of academic interest only in laser-produced plasma processes at very high intensities.

Whilst the non-linear force was splendidly reconfirmed by numerical studies and experimentally as mentioned, the effects of the non-linear optical response for very high laser intensities were well included only in the advanced numerical treatments.

5.2. Suprathermal 'Hot' Electrons and Resonances

Analysis of the spectrum of the X-rays from laser-produced plasmas at the beginning of the seventies produced highly confusing results. There were indications from some authors that the emitted bremsstrahlung corresponded to a temperature of about 100 eV as agreeing with gas dynamics, and there were other clear measurements of temperatures of 20 keV. A clarification was achieved by K. Eidmann[56], whose motivation to study the laser-produced plasmas was—as it should be noted—given by Wilhelm Walcher for application as a laser ion source. Eidmann discovered that the X-ray spectrum for a large number of frequencies could be separated into a lower temperature, corresponding to the thermal electrons, and into an elevated 'temperature' corresponding to the energetic or 'hot' electrons.

This result was repeatedly confirmed. Again an $I\lambda^2$ relation was confirmed[24] and there exist numerous qualitative suggestions as to the reason for the energetic electrons. The dielectric swelling of the oscillation energy ϵ_{osc} within the plasma of a refractive index $\tilde{n}$ is[38]

$$\epsilon_{osc} = \epsilon_{osc,vac}/|\tilde{n}| \tag{15}$$

over its vacuum value (indicated by the index 'vac'). The absolute value of the refractive index $\tilde{n}$ has its minimum at the critical density (where $\omega = \omega_p$), arriving then at maximum oscillation energies in the plasma. This value occurred in general hydrodynamic computations given by a swelling factor $1/\tilde{n}$ of 100 or in experiments with microwaves at 600. These values would be quite sufficient to explain most of the experiments[39] of energetic electrons.

But other models appeared for the explanation of the energetic electrons. One is the Försterling–Denisov[58] resonance absorption (see Chapter 11.2 of Refs. 38, 39) of which the result of Maki (see Ref. 38) was most convincing: if the fast thermal electrons of a Maxwellian distribution are moving through the very thin area of the Försterling–Denisov resonance maximum for obliquely incident laser radiation for p polarization, they can speeded up to reach the high velocities measured in the X-ray spectrum, or measured directly as the emission of energetic electrons.

The Försterling–Denisov resonance absorption[58,59] appears as a very strong longitudinal oscillation of the electrons in the plasma at the critical density when the radiation is obliquely incident with p polarization, with the maximum effect at an angle of incidence of about 20°. This can be seen from Fig. 10, where the exact Maxwellian solution of the plane-wave neodymium glass laser field obliquely incident at 26° on a plasma is evaluated. The electron density is linearly increasing from the vacuum value at $x = 0$ to the critical density at a depth of $x_o = 3.14$ vacuum wavelengths. The solid line is the square of the x-component only for the electric laser field, which corresponds to a standing wave before reaching the turning point at $x_T = 2.5$ vacuum wavelengths.

Before the turning point, the laser field is that of a nearly standing wave, as seen in the vacuum range for negative x. Within the plasma, the effective wavelength is stretched owing to the absolute value of the dielectic coefficient of less than one, and the amplitude swells in the same way and would then decay exponentially after

the last standing wave maximum. The fact that the standing-wave is not completely modulated is due to the absorption for the case of a plasma of 100 eV temperature. What is remarkable for the x-component of the field in the range of the exponential decay, and different from all the other components, is the appearance at very steep maximum of the resonance maximum at the critical density x_0.

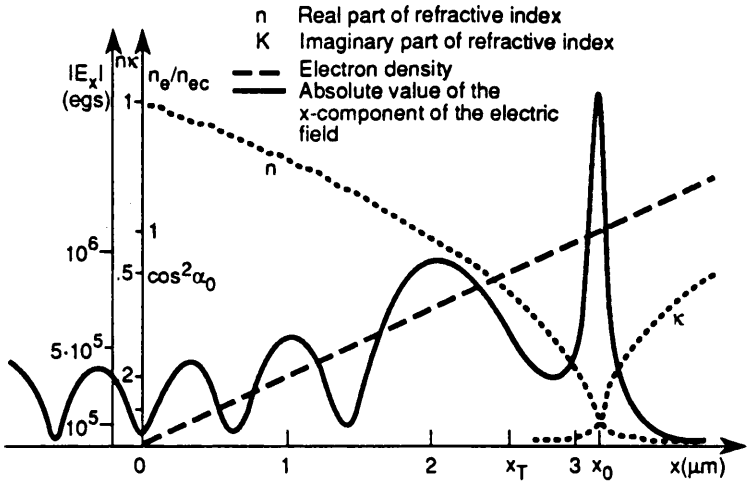

Fig. 10 26° incident p-polarized light on 100 eV hot deuterium plasma with linear density increase along the x-direction. Exact Maxwellian evaluation of the x-component of the laser E-field showing the exponential decay beyond the turning point x_T and a special maximum at the critical density x_0 according to Lädrach[39]

Whilst this result is a simple linear (Airy) solution of the Maxwellian equations, where the real and imaginary parts of the refractive index are shown in Fig. 10, the behaviour of electrons in the neighbourhood of the resonance maximum is of non-linear nature. One special result is the effective dielectric constant (Fig. 11). For a collisionless plasma, this function has a pole of minus infinity[60] at the critical density, whilst adding a very tiny amount of collisions (absorption) causes the pole to jump from minus infinity to a very high positive value[38,39]. This is one example of how important it is to take into account the collision frequency in plasmas; otherwise results can change from nearly plus infinity to minus infinity if the usual simplification of collisionless plasmas is assumed in the microscopic plasma theory (see subection 3.5 of Ref. 39).

The identification of the suprathermal electrons as being due to the oscillation caused by swelling was evident from the results on non-linear force[38]. This model was favoured by K. Brueckener, according to private discussions at the Los Alamos National Laboratory. It was shown that these electrons should not only cause the energetic X-ray signals by their oscillation, but also this oscillation energy should be converted by quiver drift into translative energy of the mentioned elevated value [Eq. (11.60) of Refs. 38, 39]. The measurements[20] of the Al^{11+} ions of about 2 MeV immediately correspond to the simultaneously measured oscillation energy of 200 keV of energetic

electrons in agreement with this model. These dielectric swelling mechanisms automatically appeared in the multi-particle simulations (using 1 million plasma particles)[59], where the processes of the polarization-dependent Försterling–Denisov resonance absorption and the quiver drift appeared automatically as well as the internal electric fields in the plasma.

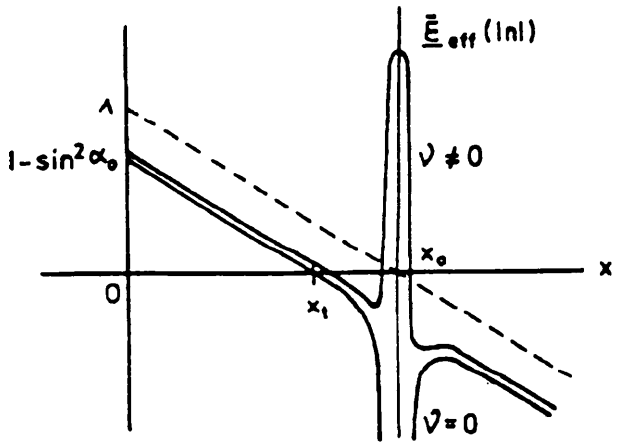

Fig. 11 The effective dielectic constant for the case of Fig. 10 without collisions (negative pole at the critical density[60] and with collisions (high positive maximum[39])

A further new resonance mechanism should be mentioned, where a similar narrow-range maximum of longitudinal oscillation in a laser-irradiated plasma is produced, as in the preceding case (Fig. 10), which may cause similar quiver drift energy gains of electrons. It was especially interesting to obtain therefore a resonance mechanism at perpendicular incidence of infinitely spread plane transversal electromagnetic waves on a plasma. This was in contrast with the Försterling–Denisov resonance, which appears only at obliquely incident light for p polarization, and several artificial explanations were needed to discuss the related anomalous absorption mechanisms in laser-produced plasmas by assuming bent surfaces, etc.

The new resonance was found from the laser light produced by longitudinal oscillation[61] of the electron gas of the plasma according to the local plasma frequency whose amplitude reaches very high values at the depth where the electron density corresponds to four times the critical density. A necessary condition is that the intensity of the laser light within this exponentially decaying area is still sufficiently large. With appropriately steep linear density profiles occurring always in Airy solutions of the Maxwellian equations, the resonance maxima can be very high and narrow (Fig. 12)[62].

Returning to the discussion of the suprathermal ('hot') electrons we underline the fact that attempts have been made to explain their origin and properties from resonance mechanisms, but the questions of isothermal and thermal motion of these energetic electrons compared with all kinds of anisotropic motion is certainly not clarified. What is convincing is the fact of the experimental determination of the X-ray

energy ('temperature T_x'?) of these electrons. A compilation of the results of 25 laboratories throughout the world is shown in Fig. 13 [24], where the dependence of this X-ray temperature is given as a function of the reduced intensity I^{**}, and the value of the wavelength λ is eliminated:

$$I^{**} = I\lambda^2 \,, \tag{16}$$

the wavelength being given in micrometres and the intensity I in W/cm^2. This fact takes into account that, for example, the oscillation energy of the electrons in the laser field (quiver energy) [Eq. (10)] for different wavelengths and intensities corresponds to the same value according to the relation (16). The thresholds for instabilities (see subsection 5.4) mostly follow the same relation as well as those of relativistic effects

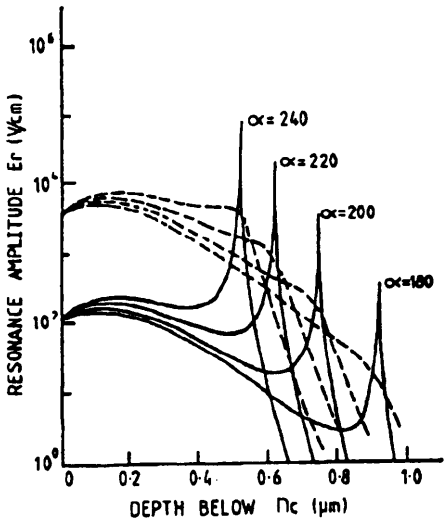

Fig. 12 Resonance amplitude of the transverse electric field vector at perpendicular incidence on a plasma within the range of usual exponential decay beyond the critical density (new resonance)[61,62]

and of relativistic self-focusing (see subsection 5.3). It is therefore no surprise, when putting together all measurements of the X-ray temperature T_x in the case of carbon-dioxide lasers, of ruby, and of neodymium glass lasers and their higher harmonics, to see that these values are nearly the same despite a difference of the wavelength squared by three orders of magnitude (Fig. 13).

Just this fact of the wavelength dependence (16) of the hot electrons can be ideally used to exclude that the measured energetic (non-thermal) ions of kilo-electronvolt and higher energies are caused by hot electrons[63]. Figure 14 is a compilation[64] of the measurements of the energetic ions up to 25 keV emitted from tantalum targets irradiated, in the one case by neodymium glass laser pulses of the same focus diameter and the same pulse duration of 30 ps with the fundamental wavelength of 1064 nm (red), and in the other case with the second harmonics (green wavelength of 532 nm). The energies up to eight times ionized ions grow linearly with the ionization Z as usual,

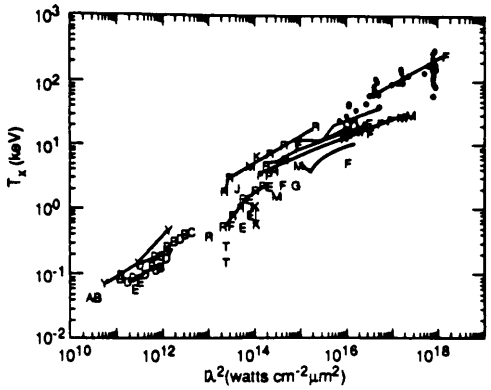

Fig. 13 Compilation of a large number of different experiments with lasers of different wavelength showing nearly the same measured 'hot' electron temperature T_x depending on the wavelength normalized laser intensity I^{**}; from Gitomer et al.[24]

but the ion energies are nearly the same though the pulse energy was 135 mJ in the red case and 30 mJ in the green case (and therefore the laser intensities have the same difference). If a hot electron mechanism, according to Eq. (16), should be valid, the green light would result in 4 times lower ion energies due to the wavelength dependence and a further 4.5 times lower values due to the different intensities (i.e. 18 times lower). Instead, the measured energies are of nearly the same value (Fig. 18). The mechanism to produce the energetic kiloelectronvolt ions is therefore not due to 'hot' electrons and has to be of a different nature.

Another criticism of an explanation of the measured energetic ions by 'hot' electrons[24] is the fact that in this latter case the appearance of 400 MeV ions with linear[20–24] increase with Z could neither be explained by a 'hot' temperature of 2 MeV nor the linear separation by Z. Any thermal Z-separation could be expected from the self-similarity model (Section 5 of Ref. 39) by recombination[65], but this relates to ion energies in the 10–100 eV range (the inner thermal core of Fig. 8 which is superceded by the 10 keV fast non-linear ions directly visible in Fig. 8) whilst megaelectronvolt ions cannot be related to the mentioned recombination mechanism.

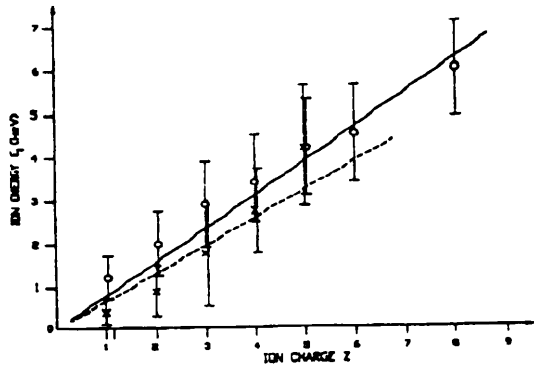

Fig. 14 Kiloelectronvolt ions of various charge numbers Z measured for a tantalum target iradiated with 30 ps pulses at the same diameter of focus with fundamental neodymium glass wavelength and 135 mJ pulse energy (o) and 30 mJ frequency doubled laser pulses (x)[63,64]

5.3. Self-focusing (Filamentation)

A crucial mechanism in laser-produced plasmas is the self-focusing of the laser beams or of several parts of it in a plasma, producing filaments of rather small beam diameter. The first self-focusing was observed when a laser beam of moderate power penetrated a dielectric medium. The second- and higher-order intensity dependent terms of the dielectric constant caused a change in the initially plane-wave fronts of the beam and normally was focused or periodically focused and defocused. The first theoretical model was published by Chiao, Garmire and Townes[66] and resulted in a threshold of laser power (not intensity) from where onwards a laser beam is self-focused. The second-order dielectric coefficients were of the same value for the laser field as measured before by electrostatics. The thresholds for dielectrics were above 10^5 W for liquids such as CS_2 and 1000 times (approximately inversely proportional to the density) higher for air.

In plasmas there is no analogous non-linear dielectric response. The basically different mechanisms of the non-linear dynamics characterized by the ponderomotive force, however, result in self-focusing in plasmas.

In order to derive the threshold for self-focusing of a laser beam in a plasma, three physical mechanisms have to be combined. Assuming that the laser beam has a Gaussian intensity profile in the radial direction while propagating in the x-direction, the generated non-linear force $\mathbf{f}_{NL}$ in the r-direction has to be compensated by the thermokinetic[67] force $\mathbf{f}_{th}$

$$\mathbf{f}_{th} = \mathbf{f}_{NL}, \quad \nabla \cdot \left(\mathbf{T} - \frac{\tilde{n}^2 - 1}{4\pi} \mathbf{EE} \right) = \nabla n_e kT(1 + Z) \tag{17}$$

where use is made of Eq. (8b). The second physical mechanism is the total reflection of the laser-beam components starting under an angle α_0 from the centre of the beam and bent into a direction parallel to the axis, owing to the density gradient of the plasma. The third condition is the diffraction requirement that the main part (for example, as defined by the first diffraction minimum) of the beam has to have an angle of propagation α, which is less than the angle of total reflection. These three conditions are sufficient to calculate the threshold.

A Gaussian density profile including the refractive index $\tilde{n}$ is described by the formula

$$\overline{E}_y^2 = \frac{e_v^2}{2|\tilde{n}|} \exp\left(-\frac{r^2}{r_o^2} \right) , \quad \overline{H}_z^2 = |\tilde{n}|^2 \overline{E}_y^2 . \tag{18}$$

Here, r_o can be interpreted as the radius of the laser beam. This is only an approximation of the exact Maxwellian formulation. The non-linear force in the direction of r is from Eqs. (8a) and (8b), using Eq. (18)[67] with a maximum value

$$\bar{\mathbf{f}}_{NL} = \mathbf{i}_y \frac{1 + \tilde{n}^2}{16\pi\tilde{n}} \frac{E_y^2}{r_o} \sqrt{2} \exp\left(-\frac{1}{2} \right) \tag{19}$$

If this has to be compensated by a thermokinetic force under the assumption of a spatially constant plasma temperature,

$$\mathrm{f_{th}} = -\mathrm{i}_y k T_{\mathrm{th}} \left(1 + \frac{1}{Z}\right) \frac{\mathrm{d}n_e}{\mathrm{d}r} \tag{20}$$

Equating this force and the non-linear force of Eq. (19) provides an expression for the electron density gradient of the plasma at the laser beam.

$$\frac{\partial n_e}{\partial y} = \frac{[2/\exp(1)]^{1/2}}{16\pi k T_{\mathrm{th}}} (1 + |\tilde{n}|^2) \frac{E_v^2}{y_o |\tilde{n}| (1 + 1/Z)} \tag{21}$$

The second physical condition of total reflection is given by the refractive index in the centre of the beam, $\tilde{n}$, and its value at y_o, for which with Eq. (21) the following expression is formulated[67]:

$$\sin\left(\frac{\pi}{2} - \alpha_o\right) = \frac{|\tilde{n}|}{|\tilde{n}_{y_o}|} \tag{22}$$

Using a Taylor expansion and a negligibly small collision frequency leads to

$$\sin \alpha_o = \left(\frac{2}{\tilde{n}} \frac{\partial \tilde{n}}{\partial n_e} \frac{\partial n_e}{\partial r} r_o\right)^{1/2} \tag{23}$$

If—as a third physical condition—a particular wave with an angle α for the first minimum of diffraction, including Rayleigh's factor 1.22, has to be reflected totally, the following condition is found:

$$\sin \alpha = \frac{1.22\pi c}{2\omega r_o} \leq \sin \alpha_o \ . \tag{24}$$

Expressing the right-hand side by Eq. (23) and using Eq. (21) and the value of the electrical laser field amplitude E_{v0} by the averaged laser power P, a laser power threshold

$$P \geq \frac{(\pi c)^2 n^3 m_e}{e^2 [2/\exp(+1)]^{1/2} c_1^2 (1 + n^2)} \tag{25}$$

is obtained, with P in watts and T in electronvolts

$$P \geq \begin{cases} 1 \times 10^6 T^{-5/4} & \text{for } \omega_p \lesssim \omega \\ 8 \times 10^3 T & \text{for } \omega_p \ll \omega \end{cases} \tag{26}$$

This was the first quantitative theory of the non-linear force self-focusing or, as it was initially called[67], the ponderomotive self-focusing. This result was rederived by several other authors[39] and fully reproduced. The same thresholds are also achieved by Chen's non-linear force treatment of the filamentation instability[68].

A further surprising result[67] is the fact that the power threshold for self-focusing in plasma is very low, in the range of megawatts or less. This is in agreement with measurements first published by Korobkin and Alcock[69]. Measurements of Richardson et

al.[70] especially demonstrated in detail that the beam centre shows a depletion of plasma. Another success of the theory is the agreement of the measured beam diameters[69] of a few micrometres for a laser power of 3 MW. If one can assume that the stationary conditions for self-focusing are reached when all plasma is moved out of the centre of the laser beam, the electromagnetic energy density $(E^2 + H^2)/8\pi$ with the electric and laser fields E and H is then equal to the gas dynamic pressure $n_e(1 + 1/Z)KT$. This is the case for densities close to the cut-off density, where the laser intensity is equal to the threshold intensity I^* of the dominance of the non-linear force. It is evident that the beam then has to shrink down to such a diameter to reach the necessary 10^{14} W/cm^2 from a laser power of 3 MW. The resulting beam diameter is then a few micrometres for neodymium glass laser radiation, in full agreement with the measurements.

This result was the first clarification of the kiloelectronvolt ion generation, Linlor effect (see subsection 5.1[39]), where (Fig. 7) for laser powers below 100 kW to 1 MW, the laser light always produced a classical heating, evaporation, and plasma generation, with typical temperatures of 20,000 to 50,000 K and with energies of the emitted ions up to about 10 eV and an electron emission with classical Langmuir–Child space-charge limitation. Contrary to this classical behaviour, laser powers above megawatt resulted in maximum kiloelectronvolt ion energies, their linear Z-dependence, and in electron emission with many orders of magnitude higher current densities. It was concluded that, for the laser powers above megawatt, self-focusing is produced. The electromagnetic energy density in the filaments corresponds to intensities above the threshold where the non-linear force is dominating over the thermal forces, and the non-linear force produces Z-dependence of the energetic ions from Eq. (15) given by

$$\epsilon_{\text{ion}} = \frac{Z}{2}\epsilon_{\text{osc.max}} \cdot \tag{27}$$

This result [see Eq. (9.25) of Ref. 39] can be explained by the quiver drift of the electrons in the laser field when moving from the filament towards the incident laser beam.

Whilst these pondermotive self-focusing mechanisms could explain the MW laser pulse threshold of the non-linear mechanisms as kiloelectronvolt ions etc., another self-focusing mechanism occurs at much higher laser intensities. It is connected with the range where the quiver motion of the electrons in the laser field reaches oscillation energies in the range of mc^2. It was shown, in several examples, that ion energies from 100 keV to a few hundred MeV could well be explained by this mechanism[71].

The relativistic change of the electron mass, due to oscillation energies close to or above $m_o c^2$ [Eq. (10)] causes a modification of the optical constants, as shown in Eqs. (5) to (7). With this relativistic intensity dependence of the absolute value of the refractive index $|\tilde{n}|$, the effective wavelength of propagating laser radiation in a plasma is then given by

$$\lambda = \frac{\lambda_0}{|\tilde{n}(I)|} , \tag{28}$$

where λ_0 is the vacuum wavelength. In Fig. 15, a Gaussian-like intensity profile of

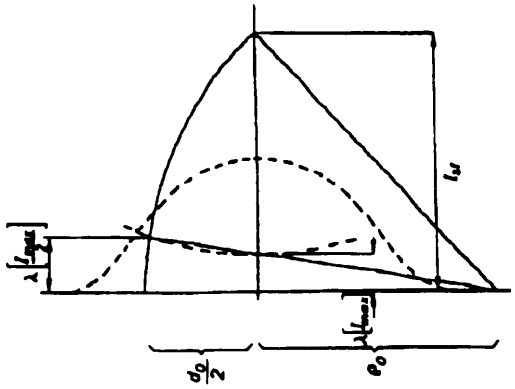

Fig. 15 Relativistic self-focusing. Geometry of a plane-wave front (vertical line) bent into the spherical (dashed) wave front owing to the relativistic mass dependence of the refractive index at various laser intensities[39,71]

a laser beam moving through a homogeneous plasma is considered. The relativistic refractive index results in the condition

$$|\tilde{n}(I_{\max})| > |\tilde{n}(I_{\max}/2)| \ , \tag{29}$$

showing that the effective wavelength (28) is shorter for the higher laser intensity in the centre of the beam than at the lower intensity of the half maximum intensity value. As shown in Fig. 15, an initially plane wave front is then bent into a concave front, which tends to shrink down to a diffraction-limited beam diameter of about one wavelength. From the geometry of Fig. 15 this shrinking can be approximated by an arc resulting in a self-focusing length l_{SF}

$$l_{SF} = \left[d_0 \left(\rho_0 + \frac{d_0}{4} \right) \right]^{1/2} \tag{30}$$

where d_0 is the initial beam diameter, and the radius of the arc with ρ_0 is given by the effective wavelengths of the various intensities. From the geometry of Fig. 15, the following relation is derived:

$$\frac{|\tilde{n}|(I_{\max}/2)|^{-1}}{(d_0/2 + \rho_0)} = \frac{|\tilde{n}(I_{\max})|^{-1}}{\rho_0} \tag{31}$$

In combination with Eq. (30), this results in the ratio of the self-focusing length related to the beam diameter[71]

$$\frac{l_{SF}}{d_o} = 0.5 \left(\frac{|\tilde{n}(I_{\max})| + |\tilde{n}(I_{\max}/2)|}{|\tilde{n}(I_{\max})| - |\tilde{n}(I_{\max}/2)|} \right)^{1/2} \tag{32}$$

Using the relativistically exact absolute value of the refractive index $\tilde{n}$ with the intensity-dependent relativistic values of the plasma frequency and the collision frequency, a numerical evaluation of Eq. (32) is given in Fig. 16 for neodymium glass laser radiation

for plasma densities $N = 0.1$ or 1.0 times the non-relativistic cut-off density value[72]. It is remarkable that the self-focusing length is as low as two times the beam diameter for 100% of the cut-off density if the laser intensity is between 10^{16} and 3×10^{18} W/cm^2. The last intensity is the relativistic threshold corresponding to an electron oscillation energy of $m_e c^2$. It is further interesting to note that the process of the relativistic self-focusing also occurs for laser intensities that are much less than the relativistic threshold, even 1000 times less. This phenomenon of the occurrence of relativistic effects at intensities much lower than the relativistic threshold was not new, as could be seen from the work concerning relativistic instabilities in plasmas[39].

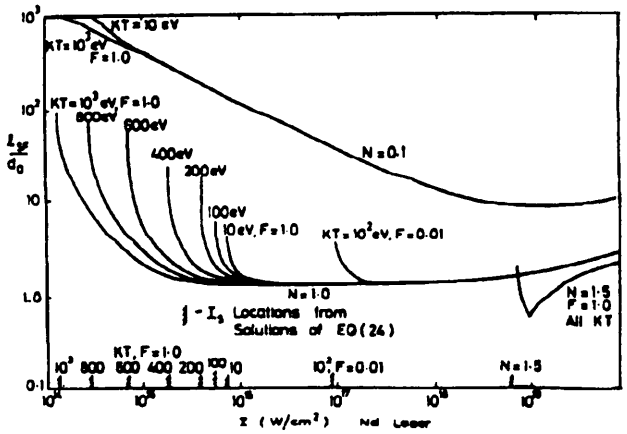

Fig. 16 Relativistic self-focusing length l_{SF} per initial neodymium glass laser intensities I of a beam diameter d_0 for critical electron density $N = 1$ and ten times less density $N = 0.1$ for different plasma temperatures T [39,72]

The relativistic self-focusing can be related to the generation of a Schrödinger soliton[73]. The subsequent acceleration of the ions in the focus will result in a smaller number of the most energetic ions in the axial direction than in the radial direction of the focus[73]. This fact was observed when the ions accelerated in a laser focus at relativistic self-focusing were measured in the place of their generation (contrary to the usual time-of-flight measurement) from the Doppler shift of the X-ray spectra of 1 to 6 Å wavelength. The P^{13+} ions of 2 MeV energy from irradiation of 2×10^{15} W/cm^2 neodymium glass laser pulses corresponded to the energies expected from the relativistic self-focusing (see Fig. 16), but showed (from the evaluation of the absolute values of the X-ray intensity) the preferential direction of the number of the emitted ions along the radius[74] as calculated[73].

The maximum ion energy was given by the simple relation [Eq. (12.54) of Ref. 39]:

$$\epsilon_i^{\text{trans}} = \frac{3}{4} m_e c^2 I / I_{\text{rel}} = 8.13 Z P \text{ MeV}, \quad [P] \text{ in TW}, \tag{33}$$

where the diameter of the focused beam, not determined theoretically (because of the paraxial approximation not fully reproducing the diffraction) was assumed to be twice the wavelength. The resulting ion energies between 0.1 and 500 MeV and the corresponding measurements agree very well (see Fig. 12.16 of Ref. 39). If the experimental

calibration of the X-ray spectroscopical measurements of Rode[23] had been used, a semi-empirical determination of the diameter of the filament, not determined theoretically, at relativistic self-focusing would have been achieved, resulting in a 0.6 times smaller diameter.

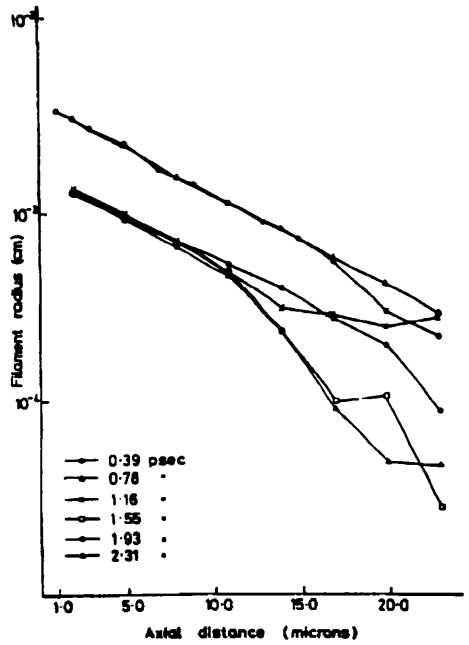

Fig. 17 A 10 TW neodymium glass laser pulse incident from the left-hand side on a Sn^{38+} plasma of initially uniform critical electron density. Evaluating the beam diameter over the depth for various times shows the relativistic self-focusing to one wavelength beam diameter after 2.3 ps [25,39]

The value of the ion energy of 400 MeV, taken from the result[24] of Fig. 5, agrees with the prediction of Eq. (33). In order to predict the maximum ion energy, if relativistic self-focusing of a kind of ANTARES laser beam of 80 TW power had been applied, it was worth while establishing a two-dimensional computation[26,72,74] of a beam in plasma of nearly critical density. If the neodymium glass laser pulse had a rise-time of 18 ps, no relativistic self-focusing occurred, because the radial non-linear force was moving out of the plasma too fast before the otherwise instantly working self-focusing could be observed. Only if neodymium glass laser pulses in the terawatt range of 5 ps rise-time were used was the relativistic self-focusing fast enough compared with the expelling of the plasma from the beam. This can be seen from the temporal development of the beam radius for various depths (Fig. 17) where the printout of the density profile (initially constant) at various times showed self-focusing. One example is given in Fig. 18. The energy gained in the motion against the laser light in the beam axis reached 6 GeV for Sn^{38+}. This value, corresponding to Eq. (33), indicates that the filament diameter of the relativistically focused beam is smaller by about a factor of 2 than assumed in Eq. (33).

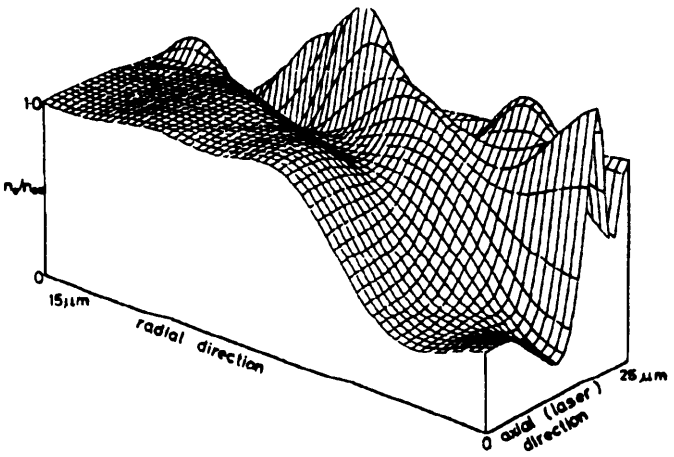

Fig. 18 Same case as Fig. 17: the initially constant critical density has been changed to the shown profile depending on the axial depth and radius at 1.16 ps [25,39]

5.4. Parametric Instabilities

Referring to the two types of resonance conditions of laser interaction with plasma explained in subsection 5.2, there is an energy-transfer of laser radiation to plasma by nearly resonance conditions as known from parametric oscillations and instabilities. These parametric instabilities consist of a number of energy-transfer processes into oscillation or wave modes of the plasma with subsequent significant phenomena. One of these mechanisms is the generation of second harmonics or of 3/2 harmonics, which provide interesting information for the diagnostics of the interaction. However, it should be underlined from the beginning that it has been shown experimentally, after very extensive studies of these instability phenomena, that their net contribution to the amount of the transfer for the laser energy to the plasma is not significant[39].

The basic phenomenon 'parametric instability' was called 'parametric resonance' when Landau discussed an oscillating mechanical system of which one parameter was influenced by another oscillation[75,76]. One example is a mathematical pendulum of length l and mass m, whose origin is oscillating in the vertical direction y by a frequency ω_0, and an amplitude A ($y = A\cos\omega_0 t$). Using the angle ϕ as the generalized coordinate, the Lagrangian (kinetic energy minus potential energy) is then

$$L = \frac{ml^2}{2}\dot{\phi}^2 + mla\omega_0^2 \cos\omega_0 t \cos\phi + mgl\cos\phi \tag{34}$$

from the Lagrange equation of the second kind

$$\frac{\partial}{\partial t}\frac{\partial}{\partial \dot{\phi}}L - \frac{\partial}{\partial \phi}L = 0 \tag{35}$$

and the following equation of motion for small amplitudes ($\sin\phi \simeq \phi \ll 1$) is achieved:

$$\frac{\partial^2\phi}{\partial t^2} + [a + q\cos(\omega_0 t)]\phi = 0 \tag{36}$$

where

$$a = \omega^2 \tag{37}$$

is the radian frequency of the undisturbed pendulum (amplitude of disturbance $A = 0$) and

$$q = \frac{4\omega^2 A}{l} \tag{38}$$

Equation (36) is Mathieu's differential equation, which has the special property of quasi-periodic (stable) and non-periodic (unstable) solutions similar to Paul's quadrupole[77].

The parametric instabilities in plasmas were first studied by Oraeveski and Sagdeev in 1961 and by Silin, Dubois and Goldman, and Nishikawa[39]. A synopsis of all these models was given by a treatment based on the non-linear force, presented by F.F. Chen[68]. This analysis of the parametric instabilities in plasmas at laser irradiation starts from the non-linear force for perpendicular incidence of infinite plane waves on plasmas whose density profile permits a WKB approximation for the solution of the wave equation, Eq. (4),

$$\mathrm{f_{NL}} = -\mathrm{i_x}\frac{1}{16\pi}\frac{\omega_p^2}{\omega^2}\frac{\partial}{\partial x}\bar{\mathbf{E}}^2 \ , \tag{39}$$

or

$$\mathrm{f_{NL}} = \frac{\omega_\mathrm{p}^2}{8\pi\omega^2}\{\mathbf{E}\cdot\nabla\mathbf{E} - \mathbf{E}\times(\nabla\times\mathbf{E})\} \tag{40}$$

Chen derived this formula from the quivering motion description found in most textbooks, where the difficulties due to the phase differences between $\mathbf{H}$ and $\mathbf{E}$ and $\mathbf{j}$[39] were not followed up (this question was cleared up later by Kentwell[39]). Chen's formulation (40) has the merit that the last term results in forces along the propagation of the laser light, whilst the first term works on any deviation from the striated structure in the direction perpendicular to that of the propagation. This permits a distinguishing between *backscattering instabilities*, due to $\mathbf{E}\times(\nabla\times\mathbf{E})$, and the *electrostatic parametric instabilities*, due to $\mathbf{E}\cdot\nabla\mathbf{E}$, which is equivalent to the $\mathbf{v}\cdot\nabla\mathbf{v}$ convection term in the equation of motion of this plasma. This non-linear force in the lateral direction of the perpendicular incident plane wave may indeed need more analysis with respect to the Maxwellian stress tensor [see Eq. (8b)]. Chen[68] was aware of some of these problems, and certain limitations of the following results may be necessary.

The *electrostatic parametric instabilities* are the result of the interaction of perpendicularly incident plane waves of laser radiation with the lateral deviations of n_e, of the electron density from its equilibrium value n_{eo}, due to the $\mathbf{v}\cdot\nabla\mathbf{v}$ term in Eq. (40). For the electrostatic oscillations the plasma frequency ω_p, Eq. (6), was due to the deviation of the electrons from their equilibrium whose oscillation is attenuated by Landau damping[78]. Bohm and Gross[79] studied the generated electrostatic waves, which have the following frequency ω_e:

$$\omega_\mathrm{e}^2 = \omega_\mathrm{p}^2 + (3/2)k_\mathrm{s}^2 v_\mathrm{th}^2 \tag{41}$$

(Bohm–Gross frequency), where the thermal electron velocity $v_{th} = 2kT_e/m_e$ determines the transport of a signal by this wave (Langmuir wave). The wave vector k_s is given by the phase velocity v_ϕ of the wave, which can be very large:

$$|k_s| = \omega/v_\phi \ . \tag{42}$$

It has to be distinguished where the laser frequency ω is a little less than ω_e in which case we have an *oscillating two-stream instability*,

$$\omega < \omega_e \ . \tag{43}$$

Density ripples in the direction of the electric laser field E_0 will then grow without propagation. The laterally uniform laser field E_0 will then interact with the space-charge field E_1 of the density rippling by the non-linear force f_{NL}

$$8\pi \frac{\omega^2}{\omega_p^2} f_{NL} = -2E_0 \frac{\partial E_1}{\partial x} \tag{44}$$

causing an increase of the ripple.

If the laser frequency is a little larger than the Bohm–Gross frequency,

$$\omega > \omega_e \ , \tag{45}$$

the *parametric decay instability* is generated. The oscillating two-stream instability does not work, and the incident wave decays into an electron wave ω_e and an ion acoustic wave ω_1. The non-linear force then acts to destroy the density perturbation n_1. However, in the frame of the moving-ion wave, the density perturbation would be at rest as in the oscillating two-stream case. Its mechanisms can again operate based on quasi-neutrality and a Doppler shift, causing a growing ion wave.

The lateral effects of the parametric decay instablilities will cause a *filamentation* or self-focusing of the laser beam in the plasma. This is based on the balance of the lateral non-linear force with the gas-dynamic pressure as used in our[67] earlier treatment of self-focusing, Eq. (19):

$$\mathbf{f}_{NL} = \nabla nkT_e \tag{46}$$

Based on a Gaussian-like density profile

$$n = n_o \exp\left(-\frac{\omega_p^2}{\omega^2} \frac{\bar{E}^2}{8\pi n_o kT_e}\right) \tag{47}$$

a threshold for self-focusing at the laser power P_0 in watts

$$P_0 = 8800 \left(\frac{\omega_e}{\omega_p}\right)^2 T \tag{48}$$

was found[68], where $[T]$ = eV. This is the same value that we had derived before[67], Eq. (26), where the mechanisms of total reflection and diffraction had been added to the balance of the forces of Eq. (17) only (see subsection 5.3).

The *back-scattering instabilities* occur from non-linear forces parallel to the direction of the wave vector **k** of the laser light, where, however, the details of the quiver motion and the phases of the initial and the induced electric and magnetic field have to be included. Again currents and velocities are produced perpendicular to **k**, reacting then with the **E** field of the laser. Whilst the electrostatic parametric instabilities are transversing the laser energy into electrostatic waves, the back-scatter instabilities result in a transversion into an electromagnetic wave of frequency ω nearly in or against the direction of k. The lateral wave ω for this coupling can be equal to ω_e (an electron plasma wave); then we have *stimulated Raman scattering* (SRS). If ω is equal to that of the ion acoustic wave, we have *stimulated Brillouin scattering* (SBS). If ω is not perpendicular to k, the density perturbation can still exist if the laser field E is sufficiently large to maintain it against diffusion. This is then called *resistive quasi-mode scattering.* If $\omega_1 = \mathbf{k}_1 \cdot \mathbf{v}_e$ or $\mathbf{k}_1 \cdot \mathbf{v}_i$, where $\mathbf{v}_e$ and $\mathbf{v}_i$ are the thermal velocities of electrons and ions, interaction with resonant particles can cause an instability. This is the *induced Compton scattering* or *non-linear Landau growth.*

What is essential is that the energy balance is fulfilled

$$\hbar\omega = \hbar\omega_s' + \hbar\omega' \,, \tag{49}$$

where ω_s is the frequency of the scattered light and ω' is the frequency of the wave excited in the plasma, and the momentum balance is given by the correponding wave vectors

$$\mathbf{k}_\omega = \mathbf{k}_{\omega_s} + \mathbf{k}_{\omega'} \tag{50}$$

Without looking into the detailed derivation, the results of the threshold and growth rate in homogeneous plasma are given in Table 1.

Table 1
Formulation of Instability Threshold and Growth rates

	Threshold	Growth Rate
SBS	$v_0^2/v_e^2 = 8\gamma_i\nu_{ei}/\omega_i\omega_0$	$\gamma_0 \simeq (1/2)\,(v_0/c)\,(\omega_0/\omega_i)^{1/2}\,\omega_{pi}$
SRS	$v^2/c^2 = (2\omega_p^2/\omega_0^2)\,(\gamma_e/\omega_p)\,(\nu_{ei}/\omega_0)$	$\gamma_0 \simeq (1/2)\,(v_0/c)(\omega_0\omega_p)^{1/2}$

where v_e are the thermal electron velocity, γ_e and γ_c the electron or ion wave damping rates, and $(\omega_p^2/\omega_0^2)(v_{ei}/2)$ is the damping rate of the electromagnetic waves. The thresholds[80] for neodymium and CO_2 lasers for intensities in W/cm^2 are given in Table 2.

Table 2
Intensity Threshold for Instabilities in W/cm^2

	Nd	CO_2
SBS	10^{13}	10^{10}
SRS	10^{13}	10^{9}
Oscillation two-stream instability	10^{13}	10^{9}
Parametrametric decay instability	10^{13}	10^{10}

The action of the back-scatter instabilities can be seen immediately from the electromagnetic waves reflected from the laser-produced plasma. The intensity of the reflected light with half frequency or the higher harmonics is much less than the incident light, which is the most direct indication that the instabilities do not grow to infinity but are limited by saturation. The use for diagnostics is very valuable.

Since a lot of attention has been given to parametric instabilities in laser–plasma interaction, it is necessary to consider these processes for the physics of the laser ion source. Restrictions of the described theory were caused by the fact that these models were based on homogeneous plasmas only, whilst extremely inhomogeneous plasmas are produced by the laser. Apart from the mechanism of the parametric excitation of plasma oscillations (SRS) by the microscopic deviation of electron densities from equilibrium, with a definite lower threshold for the laser intensity, there was the proof of the macroscopic induction of these oscillations with very large amplitudes and without any threshold derived from the genuine two-fluid model[34,81] (see subsection 5.5).

Other limitations of the parametric instabilities have been found in experiments. Wong[82] used the fact of the small back-scatter intensity as an obvious argument that the dynamics of laser–plasma interaction will not be influenced by the instabilities. This result has been confirmed theoretically by Bobin et al.[34], who emphasized that the parametric instabilities can work for neodymium glass lasers for intensities between 10^{14} and 10^{16} W/cm^2 only. Above these intensities, the non-linear force is predominant for plasma dynamics. Similar conclusions were drawn by Balescu (see Ref. 39). A more detailed analysis was given by Liu et al.[83]. The non-linear force disturbs the resonance conditions for the parametric decays. At the interesting intensities near 10^{15} W/cm^2 for neodymium glass lasers, only 1% of the absorbed radiation can go into decay modes. Under very artificial conditions, this contribution may grow to 10%.

More recent experiments elaborated these facts in more detail. It is the merit of C. Labaune et al.[84] to have demonstrated experimentally that SBS, while really existing with all the properties predicted theoretically, does not account very strongly for the energy transfer of laser radiation into the plasma. Only if very extreme and pathologically non-natural density profiles with flat plateaus of 1 mm length of laser irradiation at the neodymium glass wavelength are produced artificially is a strong amount of optical energy being transferred into the ion-acoustic waves according to SBS.

Another experimental result is that of Paul Drake[85], which demonstrated that SRS is not contributing a large amount of energy transfer at neodymium glass irradiation. The mechanism of SRS certainly exists with most of the theoretically predicted properties, especially the generation of the easily detectable 3/2 harmonics in back-scattered light, which is just due to the SRS process feeding laser energy into longitudinal electron oscillations of a frequency given by the local electron density according to the plasma frequency, Eq. (6).

5.5. *Dynamic Electric Fields Inside Plasmas and Double Layers causing Acceleration*

A rather recent development, in only the last few years, in laser-produced plasmas is to look into the problems of electric double layers and into the appearance of internal electric fields which vary dynamically within the motion of inhomogeneous plasmas with or without the further modifications due the irradiation of intense electromagnetic fields of the laser. Double layers were considered as very marginal and usually a question which could be ignored in plasmas, whilst the further consequence of internal electic fields was rather a heresy in view of the space-charge neutrality of plasmas postulated in the earlier plasma physics. The space-charge neutrality (apart from the microscopic fluctuations in ranges of the Debye lengths) is indeed fulfilled if the plasma is homogeneous. This was tacitly extended to conditions of Schlüter's two-fluid[39] and the discrepancies should not surprise us if strongly inhomogeneous plasmas are considered. As known from a comparable homogeneous metal, the generation of a space charge there disappears within a decay time of 0.1 fs. However, inhomogeneities lead to the contact potential or the properties of a p–n junction in semiconductors which need not be described by diffusion currents but are described much more simply as the result of static double layers and the subsequent internal electric fields.

It must be mentioned that the properties of plasma surfaces resulted in double layers and in the ambipolar fields in Langmuir's foundations of plasma physics[86], but this marginal question of plasmas has now turned out to be esential and of a basic nature in the inhomogeneous plasma in the Universe[87], and may even lead to very strong acceleration of particles, for example, in the solar corona etc.[88]. For static conditions, the double layer could be ideally studied in the triple-plasma devices[89].

The appearance of double layers in laser-produced plasmas[34] was basically a question of the generation of energetic ions and the action of the non-linear force. When Linlor observed the kiloelectronvolt ions suddenly appearing at laser irradiation with powers above the threshold of about 1 MW, the first idea was that the double layer at the surface may electrostatically speed up the ions to the velocity of the electrons, reaching the kiloelectronvolt ion energy from a plasma temperature of only a few electronvolts only. Apart from the question, why does this all not happen below the threshold of about megawatt laser power, another argument against this electrostatic acceleration as being the main reason for the kiloelectronvolt ions is the following: the double layer has the thickness of a Debye length and the number of ions in such a volume given by the Debye length and the laser focus cross-section may reach a value of 10^9 only. The measurements of Linlor and all the subsequent experiments with the energetic kiloelectronvolt ions[19] obtained four to six orders of magnitude higher numbers of ions.

This was the reason why the non-linear force acceleration mechanism, which was derived with the linear Z dependence of the energetic ions, needed the involvement of the ponderomotive self-focusing with the threshold of about megawatt power. But the electrostatic acceleration by the double layer in the plasma surface was well measured later[49], as proved by the identification of one group of kiloelectronvolt ions which were independent of the optical polarization. The number of such ions[49] was indeed only of the order of the expected 10^9.

Apart from this very first involvement of the electric double layer in laser-produced plasmas, another impact came from the following basic question about the non-linear force. The force density reported in subsection 5.1 was indeed the result of the space-charge neutral theory of Schlüter, which explained that the whole plasma as a block was moved by the gradients of the electromagnetic laser field. Another model arriving at the same non-linear forces was possible from a single electron description. The inhomogeneous laser field caused a quiver drift of the electrons reaching the same acceleration, as known from the non-linear force; except that the inertia was not given by that of the electrons but by that of the ions. This was the motivation for asking the question, in which way are high electric fields being built up when the laser takes the whole electron cloud for acceleration and the ions have to follow by field attachment? These electric fields could not be expected from Schlüter's model because such internal ones were intentionally neglected.

The way out was to develop a genuine two-fluid model for the fully ionized plasma, consisting of the electron fluid and the ion fluid between which a coupling by electrostatic fields is present. This holds in one spatial dimension only (expressed by Poissons's equation), and in three dimensions one has to add the complete Maxwellian equations obtaining then—apart from the 'static' electric fields—automatically in the rather complex megagauss spontaneous magnetic fields as observed in laser-produced plasmas[90]. This could all be seen from an extensive numerical evaluation[91] of the motion of the coupled two fluids, for example, of a deuterium plasma in one spatial dimension for electron densities around 10^{21} cm^{-3} corresponding to the critical cut-off density of neodymium glass laser irradiation. The numerical difficulty consists in the fact that the temporal steps have to be 0.1 fs in order to have about ten steps per fastest plasma oscillation, whilst the integration of the whole dynamic system has to arrive at several picoseconds for experimental comparison. With new developments in numerical smoothing and by derivation of a basically new mathematical system for the solution of the initial-boundary value problem[91], it was possible to solve this.

This hydrodynamic model, however, had the disadvantage that at each time step the equilibration of the energy distribution of the electrons and ions had to have Maxwellian distributions in order to follow the hydrodynamics with temperatures T of the ions and electrons. For the one-dimensional problems there were then the seven quantities for electrons (index e) and ions (index i), the two temperatures T_i and T_e, the two densities N_i and n_e, the two velocities v_i and v_e, and the x-component, E_s, of the electric field $\mathbf{E}$, all depending on x and t to be solved by special initial and boundary values. This had to be solved by the following seven differential equations: two of continuity, two of motion, two of energy conservation, and the Poisson equation. Realistic plasmas with collisions, viscosity, and the equipartition time for temperature exchange between the two fluids were included. The transverse laser field (perpendicular to x) was appearing only in the non-linear force terms with the squares of the electric and magnetic laser fields E_L and H_L as contributions to the equation of motion of the electrons and further as the heat source of collisional absorption in the electron equation of energy conservation. In order to calculate the laser field from the bound-

ary conditions of some temporal incident laser intensity, the Maxwellian equations had to be solved for the complete inhomogeneous, and dynamically developing, plasma at each time step with the boundary condition of evanescent waves only in the superdense plasma.

This real-time realistic plasma revealed plasma properties never obtained before numerically. First—without any laser—it could be seen how a plasma expands into vacuum. Figure 19 shows the evaluated longitudinal electric field E_s between the electrons and the ions for the following initial conditions: a deuterium plasma of 1 keV electron and ion temperature with zero velocity, and a density ramp (for electrons and ions the same at the beginning) growing linearly from 5×10^{18} cm^{-3} at $x = 0$ to twice this value at $x = 10$ μm. The field is then zero at $t = 0$. For growing time (given in periods of the smallest plasma frequency) a very hefty oscillation of the E field is seen. This corresponds to the fact that the electrons with their small mass leave the ramp very quickly by thermal hydrodynamic motion until they are stopped and returned by the E field. They do not return to the initial position since the ions too are moving hydrodynamically owing to their temperature and the pressure gradient, and a change in the sign of the electric field does not occur anywhere. The oscillation is then damped, and after 40 periods a nearly stationary field profile is reached. The electric fields of MV/cm are to be expected, since there is a temperature of kiloelectronvolts and a plasma decay of 10^{-3} cm.

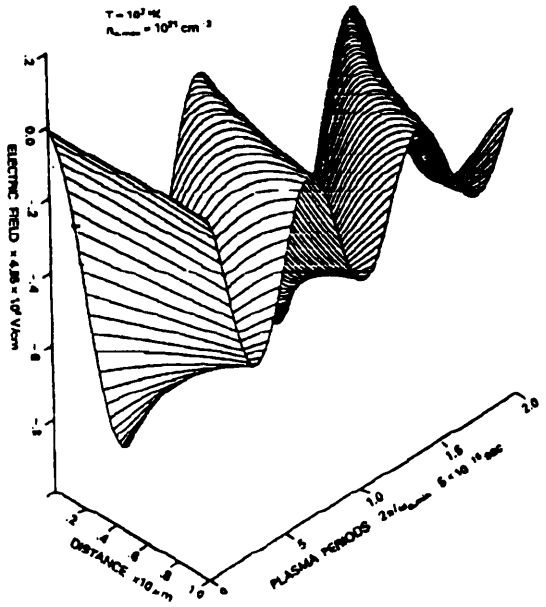

Fig. 19 Interior electric field in the x direction in a 1 keV temperature plasma at rest at time $t = 0$ with a density profile linearly growing along the distance $x = 0$ from 5×10^{18} cm^{-3} to twice this value at 0.01 mm depth. The electrostatically coupled motion of the electron and ion fluid at expansion shows the oscillating field[39,91]

Irradiating a plasma profile with a highly bent parabolic initial density profile of 25 wavelengths thickness with neodymium glass laser radiation of 10^{17} W/cm^2 intensity, the full dynamics of laser-produced plasmas appears. The generation of the density minimum (caviton) and the speeding up of the plasma to velocities of a few 10^8 cm/s against the laser light[34,91,92] can be noted within 1 or 2 ps interaction (in agreement with measurements and rough hydrodynamic estimation from the magnitude of the very strongly driving non-linear force. What can be seen, in addition, is the longitudinal electric field between the electron and ion fluid with a most complicated large amplitude (10^9 V/cm) oscillation and with the recognition of pseudo-Langmuir waves[34] (one example is given in Fig. 20). Owing to the caviton, an inverted double layer is even appearing[92], in agreement with measurements performed independently at the same time as the computations[34].

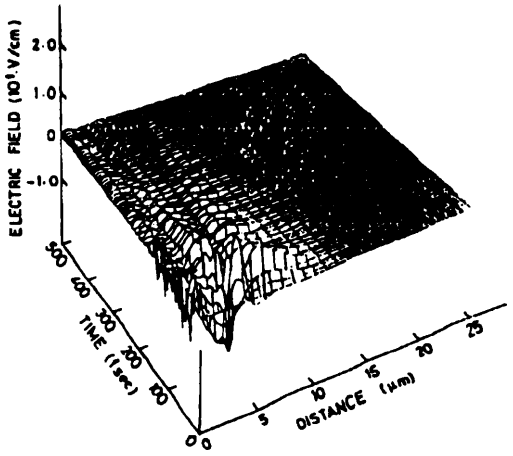

Fig. 20 Longitudinal electric field in the plasma produced by 10^{17} W/cm^2 neodymium glass laser irradiation of a 25 wavelength thick plasma slab of parabolic initial ($t = 0$) density[34]

It is evident that the longitudinal electric field is no longer a conservative electrostatic field. Any closed-loop path integration of this highly time-dependent $E_s(x, t)$ is then different from zero. One example of this method of energy gain and automatic acceleration of electrons within such an inhomogeneous plasma is shown in Fig. 21 for an initial parabolic density profile as described before[34]. An electron is assumed to start to move from $x = 7$ μm against the laser light (coming from $x = 0$) with initial energies of 1, of 5, and of 30 keV. The energy which the electron gains during this motion is plotted in Fig. 21. We see that the electrons can be speeded up to 140 keV energy when leaving the plasma at the side of the laser irradiation. However, a slowing-down could well occur resulting in a motion into the reverse direction, and the 5 keV electron, for example, is then stopped at about 1.2 μm at the time when the other electrons are leaving the plasma.

This case was only an illustration that it is necessary to be aware of these complex acceleration mechanisms of particles in laser-produced plasma in addition to all the

numerous mechanisms mentioned before. The double-layer mechanisms have several basic consequences, for example in stabilizing surface waves from the surface tension which is a result of the electric fields in the double layers. Even the generation of surface tension in metals can be explained by this plasma model of surface tension reproducing the measured values[93] (without the difficulty of negative values as known from the jellium model) in a straightforward way, when the (then degenerate) electron gas—as in the case of a plasma—likes to leave the ions until the generated electric field produces the double layer defining the thermionic exit potential for the electrons. Whilst this potential is given by the Fermi energy, that of the low-density high-temperature plasma is simply given by kT.

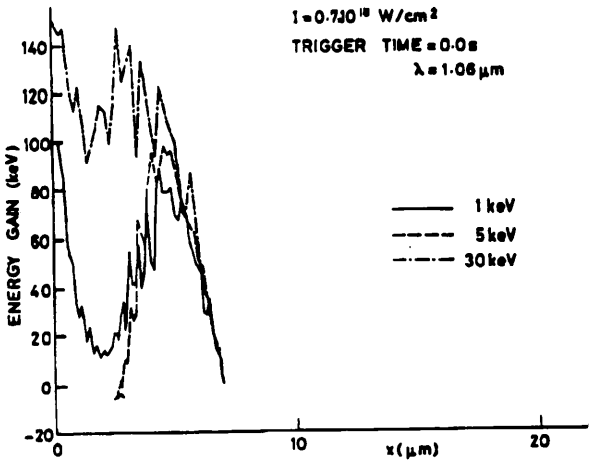

Fig. 21 Similar case to Fig. 20, but for 7 times higher laser intensity. Electrons are moving in this dynamic field from the depth of 7 wavelengths in the plasma towards the laser light with three different initial energies. The energy gain of the electrons can be more than 140 keV owing to the laser-driven dynamic electric fields[39]

This first derivation of surface tension of plasma due to the electrostatic energy in the double layer per surface area[34] was rather a surprise in plasma theory because any analogy with the case of the dipole-saturation-produced surface tension in liquids cannot be applied to fully ionized plasmas. Nevertheless, there were observations in plasmas that surface tension may work. This was seen, for example, from the smooth surface of the plasma produced by lasers from a solid target. Another case is related to the field of this article: studies of the duoplasmatron showed plasma generation on surfaces which evidently could be interpreted as surface tension[94], though the theoretical background was not derived when this was observed.

The electric fields are therefore essential inside all inhomogeneous plasmas, and, if these are hydrodynamically moving, the field is a complicated spatial and temporal function. A rather general local approximation of this field is given by the following equation[34,62]:

$$
\begin{aligned}
E_s \;=\; & \frac{4\pi e}{\omega_p^2}\left[\frac{\partial}{\partial x}\left(\frac{3n_i kT_i}{m_i}+Zn_i v_i^2\right)-\frac{\partial}{\partial x}\left(\frac{3n_e kT_e}{m_e}+n_e v_e^2\right)\right. \\
& \left.+\frac{1}{m_e}\frac{\partial}{\partial x}\frac{(E_L^2+H_L^2)}{8\pi}\right]\left[1-\exp\left(-\frac{\nu}{2}t\right)\cos\omega_p t\right] \qquad (51) \\
& +\frac{\omega_p^2-4\omega^2}{(\omega_p^2-4\omega^2)^2+\nu^2\omega^2}\frac{4\pi e}{m_e}\frac{\partial}{\partial x}(\bar{E_L^2}+\bar{H_L^2})\cos 2\omega t \\
& \frac{2\nu\omega}{(\omega_p^2-4\omega^2)^2+\nu^2\omega^2}\frac{4\pi e}{m_e}\frac{\partial}{\partial x}(\bar{E_L^2}+\bar{H_L^2})\sin 2\omega t\,,
\end{aligned}
$$

where the classical Langmuir[86] ambipolar field as a gradient of nkT is appearing for the electrons. In addition to this, however, very many more terms have been derived[34,62] including a pressure (in the first term) given by the gradient of $E_L^2 + H_L^2$, which can then be realized not as a ponderomotive 'potential' but in general as a non-conservative expression. All these pressures, including the trivial ambipolar one (first square bracket of first term), are then not constant, as in the case of Langmuir, but (apart from a constant basis) are oscillating with the local plasma frequency damped by the collision frequency. The last term, which is important only where gradients of the laser field energy density appear, is the reason for the 'new resonance' we mentioned in subsection 5.1 (Fig. 12) at four-times the critical density[61]. The term before is the reason for the high-intensity second-harmonics emission of laser radiation from the irradiated plasma corona with nearly the same intensity at very low as at high plasma density, and with some spatial periodicities. This unique second-harmonics emission, which cannot be understood from instabilities and anomalous resonances but simply and qualitatively reproduced from the mentioned term, has been measured by Aleksandrova et al. and by Gu Min et al. (see Ref. 39). These mechanisms should be taken into account, in addition to all the complications of laser interaction with plasmas mentioned above, if the processes of the laser ion source are being studied.

5.6. Pulsating (stuttering) Interaction and Smoothing

We are now reviewing a very important phenomenon which was only discovered during the last few years, but whose initial appearance goes back to the early seventies. These results may, in retrospect, modify or complement the preceding subsections, especially with respect to the energetic ion generation from self-focusing. However, most of these mechanisms are now undergoing deeper and very necessary clarification, which may have immediate consequences for studying well-defined physics questions in order to further develop the laser ion source.

The new phenomenon is the temporal pulsation of laser–plasma interaction with a fully stochastic 'period' between 10 and 50 ps. This result was gained entirely empirically[95] from a phenomenon of a spectral modulation of light reflected from laser-produced plasmas. It seems that this is a very basic phenomenon which was just not known as one—or perhaps the essential—reason for the most complicated behaviour of laser-produced plasmas.

It was well known during all the 30 years of research on laser-produced plasmas, since the laser was discovered, that the interaction is very complex. This appeared especially with the broad stream of research on laser–plasma interaction with the aim of inertial-confinement fusion. A number of the strange observations were known as the energetic ions, or their non-linear expansion (Fig. 8), or the suprathermal electrons apart from the thermal ones, and they were repeatedly confirmed before the large-scale laser fusion projects were initiated in 1972. Nevertheless, it was rather a surprise when the laser fusion experiments in the mid-seventies showed all kinds of these and other confusing anomalies, which were frustrating and delayed the hope of an easy solution of fusion energy from lasers. One way out was the indirect drive introduced by Nuckolls[96], where the laser energy is first converted into X-rays and the driving of the compression and heating of the fusion pellet is then done by the X-rays. These are then rather smooth compared with the direct drive interaction of the laser irradiation.

The difficulties of the laser–plasma interaction were mostly considered as due to the parametric instabilities, such as stimulated Raman or Brillouin scattering, SRS and SBS (see subsection 5.4). Whilst these mechanisms are evident from diagnostics and can be used actively to determine the plasma properties, it took a long time to prove experimentally that SRS[85] and SBS[84] are not dominating the energy transfer from the laser to the plasma. The question was then, what is the reason for the confusing results?

First indications go back to 1973. There were the computations of laser interaction with plasma, including the non-linear forces as well as non-linear optical constants with collisional absorption and including the exact Maxwellian solution of the laser field in the irradiated plasma corona. This was showing temporal and spatial variation of propagating- and standing-wave field components depending on the whole plasma dynamics. Initially the laser light penetrated up to the critical density, as expected, was reflected there and resulted in a net reflectivity of a few per cent. What happened next at high laser intensities was that the non-linear (ponderomotive) forces[39] pushed the plasma into the nodes of the rigid standing wave of the coherent plane-wave laser field within 2 ps, and after the plasma reached a speed of a few times 10^7 cm/s within 2 ps, the generated density ripple acted as a self-produced ideal Bragg–Laue grating. This reflected the laser light by nearly 95% within the very low density in the most peripheric plasma corona (Fig. 10.10 of Ref. 39 from the computations of 1973).

Such a reflection phenomenon was then observed by M. Lubin in 1974[91]. In that experiment the reflectivity of a laser-irradiated plasma oscillated irregularly from a few per cent to nearly 100% and back to a few per cent, etc., within 10 to 40 ps [97]. Exactly the same pulsating reflectivity was reproduced by Maddever et al.[95], and the fact was even confirmed experimentally that the location of the reflectivity in the case of a low percentage is at the critical plasma density, and for a high percentage of reflection it is located at the very low density of the outermost part of the plasma corona[95]. It was observed that the plasma gets a push to the velocity of about 2×10^7 cm/s within a few picoseconds and has no acceleration until about 15 ps later when another push comes from the laser light by a further interaction, etc. This was the long-searched for clarification as to why the spectrum of back-scattered radiation had a spectral

(stochastic) modulation of about 4 Å[95], corresponding to the repeated pushing of the stepwise plasma acceleration.

This behaviour could be reproduced exactly numerically from a very detailed hydrodynamic model. After the standing wave produced the density ripple, no light penetrated the corona and the ripple relaxed hydromechanically until about 8 ps later when light could penetrate again to the critical density, causing again a density ripple, Laue reflection, stopping of the acceleration, etc. (Fig. 22)[39,98]. The computed velocity diagrams show similar pulsation of the velocity in steps according to the 8 ps pulsation or stuttering, but, in addition, it can be recognized that, between each of the rippling processes, the velocity at the initial point of laser incidence receives a step in the range of 10^7 cm/s, as observed from the Doppler-modulated spectrum[95].

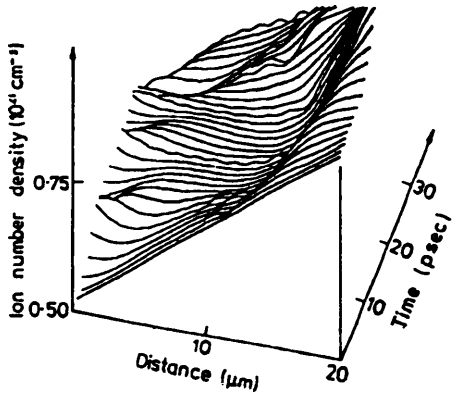

Fig. 22 Ion density in an initial 30 eV deuterium plasma with initial linear density profile at a neodymium glass laser irradiation of 10^{15} W/cm^2 from the left-hand side developing in time using the very general real-time genuine two-fluid model, where a rippling appears nearly periodically about every 8 ps[98]

The same pulsation was observed in another experiment for the 3/2 harmonics scattering (Guilietti[99]) and for other phenomena such as the double-layer potentials or the H-α emission[100]. The very sophisticated proof of this explanation of the pulsation can be based on experiments which were intuitively motivated, and performed many years ago—in 1973—after the computational result of the self-generated Laue grating. Putting a question mark in the laser beam[101] it was shown that it was reflected on the top, indicating that there was a phase-like reflection and no mirror-like reflection. The better resolution of the experiment[102] showed, however, that the question mark was jumping up and down in a period of about 25 to 30 ps. This curiosity can now be simply explained after knowing the pulsation and rippling. As long as the light with low reflectivity moves to the critical density, it is regularly mirror reflected. When the density ripple is generated at high reflectivity every 8 to 25 ps, we expect phase reflection with the question mark on top. The repetition of this experiment with better time resolution will be most interesting, not only with respect to fusion research but also for the laser ion source. The jumping of the question mark can just be used as a

test to see if there is still a stuttering, or when abolishing the stuttering as explained in the following.

The way to solve all these complex observations is obtained by the smoothing of the laser beam. These techniques were indeed suggested to overcome another problem[103]. The motivation was to achieve a very lateral uniformity in the laser intensity across the laser beam and to avoid filamentation and self-focusing (subsection 5.3). It was discovered empirically earlier, without knowing the details of this pulsation process. The use of the random-phase plate[103], or of the induced spatial incoherence (ISI)[104], or of the fly-eye lens array[105], or of the spatial spectral dispersion[106] caused, for example, a coherence of the light only for 2 ps. The consequence is that the standing waves were not fixed but washed out by the laser itself, and no Bragg–Laue grating could be generated with all its consequences. Subsequently, the pulsating 3/2 harmonics changed into a smooth emission[99] when a random-phase plane was used, or a very smooth picture of the light reflected from a target was seen with the smoothing techniques, contrary to the very granulated picture without smoothing. This smooth interaction may be the long-expected physics solution of direct-drive laser fusion[34,42].

For the acceleration in the laser ion source the process of stuttering and its suppression by the smoothing may be of great importance. This refers especially to the mechanism of self-focusing of laser beams in plasmas and whether this is the reason for an explanation of the measured kiloelectronvolt and megaelectronvolt ions[39] (subsection 5.3).

It was indeed known that the relativistic self-focusing[71,72] needed an interaction of about 10 ps or less for neodymium glass laser pulses[75] and of 70 ps for intense carbon-dioxide laser pulses[107]. Without the pulsation, detected so much later, the essential presumptions for the ponderomotive[39,61] and for the relativistic self-focusing[39,71] would not have been fulfilled. The result of the agreement of the models with the measurements (linear Z-dependence, result of 20 keV ions from plasma of about 100 eV temperature, isotropic generation of megaelectronvolt ion energies) was convincing, but the explanation of the pulsation was lacking.

Fortunately, there are now measurements available—which were in no way influenced by the new aspects of the pulsation—which were performed for studies of the laser ion source and may just meet the results expected for the pulsation without smoothing. The measurements[64] were performed with neodymium glass laser pulses of the fundamental frequency (red) or for the second harmonics (green) of a few mJ to 10 J energy for durations of between 30 ps and 3 ns irradiated on plane tantalum and other targets in vacuum. The merit of the long years of the project[64] was not only to clarify, for the first time, many problems concerning the laser ion source with respect to the extraction of the ions from the plasma plume by electric fields and with respect to recombination; but also the large amount of very systematic measurements of ion energies, using various ion analysers apart from the time-of-flight diagrams, should result in a large stock of empirical results for a wide range of parameters and for reliable comparisons of cases of various laser energies and intensities, various pulse duration, and for the fundamental and for the double laser frequency.

Some remarks are necessary firstly about the determination of the focus spot in the experiments. Its geometric extent was determined with rather low accuracy from the far field pattern of the beam, as in the usual cases where high acuracy was not necessary. It was very important to always use the same conditions when comparing ion emission from focal spots for laser pulses of different duration and different energy. For the relative comparisons, the error of the focal dimension is compensated. The following results and their relative high acuracy of comparison are the best proof of the validity of this fact.

Figure 23 shows the energetic ion energies (keV) emitted from a tantalum target when irradiated by second-harmonics neodymium glass pulses with exactly the same focus geometry. In one case the laser pulses are of 30 ps duration and of 60 mJ energy, and in the other case their duration is 3 ns and the energy 6 J, such that, in both cases, the laser intensity is the same. What is an enormous surprise is that the ion energies depending on the ionization number Z are the same in both cases, though the laser pulse energy is *one hundred* times higher in one of the cases. It would have been expected that the hundred times higher laser energy should produce a very much higher ion energy. For the slow thermal plasma following the kiloelectronvolt ion, there is indeed a drastic difference, as expected, and a secondary ion stripping process occurs for the long pulses with the existing high-density plasma plume in front of the target compared with the short pulse case.

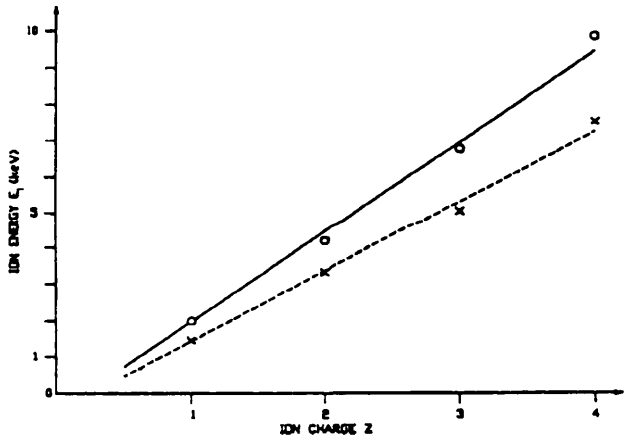

Fig. 23 Kiloelectronvolt ions of various charge number Z from neodymium glass laser irradiated tantalum at the same intensity $I = 4 \times 10^{13}$ W/cm^2 for pulses of 30 ps duration and 60 nJ energy (x) and pulses of 3 ns, 6 J (o)[63,64]. In spite of the 100 times higher energy input, the keV ions have nearly the same energy, as explained by a 30 ps pulsation mechanism

But what seems to be so ideal is that the identity of the fast ion energies for 30 ps and 3 ns may exactly confirm the pulsation for the fast ion acceleration. In the case of the 30 ps just one acceleration mechanism involving ponderomotive self-focusing (as described in subsection 5.3) may have produced the linearly Z-dependent kiloelectronvolt ions. For the long pulses, the same thing happens in the first 30 ps; then the non-linear force interaction is interrupted until within another about 30 ps

another ion generation appears, being stopped again, and a further one about 30 ps later, etc. The only difference for long pulses with the same fast ion energies may be that the number of ions is drastically larger, but this has not been evaluated since nobody involved in the experiment could have dreamed about the pulsation mechanism.

We may further conclude that in the 2 MeV ion experiments with the relativistic self-focusing by Rode[23], the same stuttering has occurred. One conclusion would be that when using smoothing for suppression of the stuttering, a basically different behaviour from that shown in Fig. 23 may be expected. Perhaps the megaelectronvolt ions in the case of Rode[23] disappear completely. Any conclusion on the physics of this question should be postponed until results are available. What it would mean practically for use in a laser ion source will be another issue. Perhaps there are simple pragmatical reasons either to use smoothing or to avoid it, depending on whether energetic or thermal ions are better for the purposes of ion extraction and injection into linacs or into the cyclotrons for pre-amplification.

6. Consequences and Possibilities of the Laser Ion Source

The very comprehensive description of the physics of laser interaction with plasmas—in view of the wealth of knowledge (mostly gained from laser fusion studies) of the field, this is still a short review—was necessary to prepare the reader of this article to appreciate how extremely complex the physics of the laser ion source is. Already the first small steps in developing the laser ion source for large accelerators (see Section 4) were so very promising in obtaining at least about 100 times higher numbers of ions per pulse in synchrotrons than before, that they may justify more extensive consideration for the laser ion source. In addition, the experimental results of a very large transfer of optical energy into nearly megaelectronvolt highly charged ions at higher laser intensities will be another considerable advantage for the laser ion source to come, with a possible further strong increase of the ion number and very high charge state.

The extensive explanation of physics phenomena in Section 5 contained some remarkable results for the understanding of some of the confusing experimental observations. It seems to be clarified now that the threshold of changing from the classical thermokinetic plasma behaviour at laser irradiation below 1 MW to the non-classical behaviour at higher powers, with the sudden appearance of kiloelectronvolt ions, coincides with the ponderomotive self-focusing threshold[67], explaining the observed diameters of the filaments and the generation of optical-energy densities above the thermal ones such that the generation of the kiloelectronvolt ions and their linear separation by the ion charge Z can be explained.

It further seems to be clarified that the relativistic self-focusing, beginning at 10^{15} W/cm^2 for neodymium glass laser radiation and at a hundred times lower intensity for carbon-dioxide lasers, reaches the measured ion energies in the range of 0.1 to 500 MeV and their linear Z-dependence, as well as their preferential emission in the radial direction as explained by a Schrödinger soliton mechanism[73]. A special success was the explanation of all these measured megaelectronvolt ion energies and radial emission

preference from the X-ray spectroscopical diagnostics of A. Rode[23]. Furthermore, all the ion energies up to 400 MeV measured by different laboratories could immediately be explained by the relativistic self-focusing, and predictions to 6 GeV ion energies with remarkably high current numbers of ions appear quite serious[74].

Nevertheless, these successes are a very first step only. In reality, the whole physics is very complex. It is necessary not only to look at the megawatt threshold or the maximum ion energy, but also at the whole spectrum of energetic (suprathermal) ions, at their specific angular dependence, at their interaction with the neighbouring plasma or target material, and last, but not least, also at the remaining thermokinetic part of plasma following the energetic part. It would indeed be naive to expect a description from a one-dimensional gas-dynamic model to reproduce all these phenomena though—as shown from the central part of the plasma of Fig. 8 [46]—the low energy part can well be followed up by gas-dynamic models for low (i.e. below about 1 keV) temperatures and moderate laser pulse energies, and even a separation of the ions of less than 100 eV energy by their charge number may well be covered by a thermal recombination mechanism[65]. For a complete attempt to cover the thermal and non-linear mechanisms, the computations of Siegrist[108] or the very sophisticated two-dimensional computations by Kane et al.[72,74] are only a first step. These computations are hydrodynamic only, and cannot cover the processes of anisotropic and non-Maxwellian energy distributions as covered by kinetic theory. The application of this theory to the problems, however, can be done for specific questions only, whilst a general computation is far beyond the present computer capacities.

For an experimental research programme, some significant new phenomena need to be clarified, which may be made in a punctual way, as, for example, the inclusion of the pulsing interaction (see Subsection 5.6) by using or avoiding the smoothing techniques. Another interesting point would be to study directly the self-focusing properties. The use of such clear experimental conditions, as in the work of the Korschinek group[64], for distinguishing the same conditions for different wavelengths, will furthermore result in numerous clarifications of several of the complex physics questions. In view of these new results, an extension of the otherwise well-developed experimental diagnostics of the emitted ions, their energy spectra, their direction dependence, their space charge, and recombination effects may be another stimulant.

Also of interest are the ion extraction mechanism and guiding into linac preaccelerators[28] or cyclotrons (Fig. 6), and the application of the extensive knowledge available from accelerator physics. Since there are new parameters to be treated now that were not available before, with much larger ion numbers and higher ion current densities, shorter pulses, etc., even this classical accelerator knowledge may need an extension towards space-charge effects, recombination (even three-body recombination as known from laser-produced plasmas), and problems of luminosity.

The proved success of the laser ion source, even for particularly low power laser installations at Dubna[29,32,33] and at the Institute of Theoretical and Experimental Physics in Moscow[28] may justify an extensive programme to specifically study the physics and the engineering development of the laser ion source. In view of the fact that

accelerators costing several thousand million dollars are involved, the use of ion (and lepton) sources, with lasers providing several orders of magnitude better ion pulses, may well justify a specific programme of several million dollars. The review given in this article of the future developments of the various ion sources may support the opinion that no miracles can be expected from improvements of the existing classical plasma ion sources. On the other hand, no total guarantee can be given for the laser ion source at the moment, apart from ecouraging improvement by orders of magnitude. However, the necessary development of large lasers with high repetition rate, high energy, and very high intensity pulses, has greatly matured, so that a not-too-expensive solution can be envisaged for a completely reliable laser ion source, functioning well for years.

Acknowledgements

The authors are grateful to several CERN staff members and visitors for stimulating discussions about this topic; especially Y. Armidouche, C. Hill, A. Kuttenberger, K. Langbein, R. Matulieniene, J. Sellmair, B.Yu. Sharkov, T.R. Sherwood, A.V. Shumshurov, C.S. Taylor, and B. Williams. Thanks are also due to T. Henkelmann and G. Korschinek of the Technological University, Munich, to V.V. Apollonov of the Institute of General Physics, Academy of Sciences of the USSR, Moscow, to V.B. Baranov and A.P. Strelzov of the Troitz Branch of the Kurchatov Institute in Moscow, and to Yu.A. Bykovski, Yu.P. Kosyrev, K.A. Monchinski, and Yu.Z. Oganesian at the Joint Institute for Nuclear Research, Dubna.

References

1. M. von Ardenne, *Atomkernenerg.* **1** (1956) 2015.
2. H. Gutbrod and H. Stöcker, *Sci. Am.* **265** (1991) 32.
3. H. Haseroth *The CERN Heavy Ion Program*, Report GSI/90/29, ISSN 0171/4546 (1990).
4. H. Schopper, *Nova Acta Leopoldina (NF)* **63**, No. 272 (1990) 79.
5. C. Rubbia, *Rev. Mod. Phys.* **57** (1985) 699.
6. C. Rubbia, Letter to CERN Staff, 8 Jan. 1992; H. Schopper, *Phys. Bl.* **47** (1991) 907; J. Ellis, *New Sci.* **131** (1991) 43.
7. H. Hora, *Plasma Model for Surface Tension of Nuclei and the Phase Transition to the Quark-Gluon Plasma*, CERN-PS/DL-Note 91/05 (Aug. 1991); S. Eliezer A. Ghatak and H. Hora, *Equations of State* (Cambridge Univ. Press, Cambridge, 1986).
8. W. Scheid, R. Ligensa and W. Greiner, *Phys. Rev. Lett.* **21** (1969) 1479; W. Scheid, H. Müller and W. Greiner, *Phys. Rev. Lett.* **32** (1974) 774; J.A. Maruhn, *High Pressure Equation of State*, Enrico Fermi Varenna School No. 113, eds. S. Eliezer and R. Ricchi (North Holland, Amsterdam, 1991), p. 507.
9. J.G. Brown, *The Physics and Technology of Ion Sources* (John Wiley, New York, 1989).
10. H. Azechi et al., *Laser & Part. Beams* **9** (1991) 193.
11. W. Lotz, *Z. Phys.* **216** (1968) 241.
12. C.M. Lyneis, *Proc. Int Conf. on ECR Ion Sources and their Applications*, ed. E. Lansing, NSCL Rept. No. MSUCP-47, (1987), p. 42; Zunqui Xie et al., *Rev. Sci. Instrum.* **62** (1991) 775.
13. G. Melin, F. Bourg, P. Briand, J. Debernardi (etc)..., J. Phys. (France) Colloq. Cl, **50** (1989) 673.
14. H. Haseroth, A. Lombardi and M. Weiss, *Feasibility for a Lead Ion Injector for the CERN Accelerator Complex*, IEEE Part. Accel. Conf. Washington (1987).
15. D.J. Warner, *Heavy Ion Acceleration using Drift-Tube Structures with Optimized Focusing*, Proc. Linac Accelerator Conference, Newport News, Virginia (1988), p. 109; U. Ratzinger et al., *The Upgraded Munich Linear Heavy Ion Post Accelerator,* IEEE Part. Accel. Conf., Washington (1987).
16. H. Haseroth (ed.) et al., *Concept for a Lead-Ion Accelerator Facility at CERN*, CERN 90-01 (1990).
17. K.-D. Linsmeier, *Bild Wiss.* **12** No. 2 (1992) 26.
18. D. Lichtman and J.F. Ready, *Phys. Rev. Lett.* **10** (1963) 342; J.F. Ready, *Effects of High-Power Laser Radiation* (Academic Press, New York, 1971);
    R.V. Artyunyan et al., *Laser Beam Effects on Materials* (in Russian) (Nauka, Moskow, 1989).
19. W.I. Linlor, *Appl. Phys. Lett.* **3** (1963) 210.
20. A.W. Ehler, *J. Appl. Phys.* **46** (1975) 2464.
21. Yu.A. Bykovskii, N.N. Degtyarenko, V.F. Elesin, Yu.P. Kozyrev and S.M. Silnov, *Sov. Phys.-JETP* **33** (1971) 706; V.V. Apollonov et al., *JETP-Lett. (USA)* **11** (1970) 252.

22. M. Siegrist, B. Luther-Davies and J.L. Hughes, *Opt. Commun.* **18** (1976) 605.
23. A.V. Rode, Dissertation, Moscow, 1983; N.G. Basov, K. Götz, A.M. Maksimchuk, Yz.A. Mikhailov, A.V. Rode, G.V. Sklikzkov, S.I. Fedotorov, E. Förster and H. Hora, *Sov. Phys.-JETP* **65** (1987) 727.
24. S.J. Gitomer, R.D. Jones, F. Begay, A.W. Ehler, J.F. Kephart and R. Kristal, *Phys. Fluids* **29** (1986) 2679.
25. F. Begay, W. Ehler, A. Hauer, S.R. Goldman and G.R. Magelssen, *Observation of High Energy Heavy Ion Velocity Distribution in CO_2 Laser-generated Plasmas*, 13th Annual Anomalous Absorption Conf., Banff, June 1983, Los Alamos Nat. Lab. Report LA-UR-83-1603.
26. D.A. Jones et al., *Phys. Fluids* **25** (1982) 2295.
27. Y. Armidouche, H. Haseroth, A. Kuttenberger, K. Langbein, J. Sellmair, B. Sharkov, T.R. Sherwood and B. Williams, *Rev. Sci. Instrum.* **68** (1992) (in the press).
28. B.Yu. Sharkov et al., *Rev. Sci. Instrum.* **68** (1992) (in the press).
29. K.A. Monchinski (Dubna), private communication, April 1991.
30. N.J. Peacock and R.S. Pease, *J. Phys.* **D2** (1969) 1705; H. Hora, J.C. Kelly, J.L. Hughes and B. Luther-Davis, US-Patent 4,199,685 (1980).
31. T. Omari, M. Katsurai and T. Sekiguchi, *Jpn. J. Appl. Phys.* **19** (1980) L728; R.H. Hughes, D.O. Pederson and X.M. Ye, *J. Appl. Phys.* **51** (1983) 4088; G. Korschinek and J. Sellmair, *Rev. Sci. Instrum.* **57** (1986) 745.
32. V.B. Kutner, Yu.A. Bykovsky, V.P. Gusev, Yu.P. Kozyrev and V.D. Peklenkov, *The Laser Ions Source of Multiplicity Charged Ions*, Conference Summary, Dubna, 1990.
33. L.Z. Barabash, Yu.A. Bykovsky, A.A. Golubev, Yu.P. Kosyrev, D.G. Kosharev, K.I. Krechet, Yu.I. Lapitskii, S.V. Latyshev, R.T. Haydarov, B.Yu. Sharkov and A.V. Shumshurov, *Laser & Part. Beams* **2** (1984) 49.
34. S. Eliezer and H. Hora, *Phys. Rep.* **172** (1989) 339; J.L. Bobin, *Phys. Rep.* **122** (1985) 173.
35. M. Key, *Phys. World*, No. 8 (1991) 52.
36. R.A. Mayers, ed. *Encyclopedia of Physical Sciences and Technology* (Academic Press, New York, 1986), Vol. 7, p. 99.
37. H. Hora, *Laser Plasmas and Nuclear Energy* (Plenum, New York, 1975).
38. H. Hora, *Physics of Laser Driven Plasmas* (John Wiley, New York, 1981).
39. H. Hora, *Plasmas at High Temperature and Density* (Springer, Heidelberg, 1991).
40. H.G. Ahlstrom, *Physics of Laser Fusion* (Nat. Tech. Inf. Service, Springfield, Va., 1983).
41. N.G. Basov, Yu.A. Zakhaerenkov, N.N. Zorev, A.A. Rupasov, G.V. Sklizkov and A.S. Shikanov, *Heating and Compression of Thermonuclear Targets by Laser Beams* (Cambridge Univ. Press, 1986).
42. G. Velarde, J.M. Martinez-Val and A. Ronen *Inertial Confinement Energy* (IRC, New York, 1992).
43. J.F. Ready, *J. Appl. Phys.* **36** (1965) 462.
44. R.E. Honig, *Appl. Phys. Lett.* **3** (1963) 8.

45. N.R. Isenor, *Appl. Phys. Lett.* **4** (1964) 152; H.J. Schwarz, *Laser Interaction and Related Plasma Phenomena*, eds. H. Schwarz and H. Hora (Plenum, New York, 1971), Vol. 1, p. 207.
46. A.G. Engelhardt, T.V. George, H. Hora and J.L. Pack, *Phys. Fluids* **13** (1970) 212; H. Hora, *Laser Interaction and Related Plasma Phenomena*, eds. H. Schwarz and H. Hora, (Plenum, New York, 1971), Vol. 1, p. 273.
47. N.G. Basov, and O.N. Krokhin, *3rd Int. Quantum Electronics Conference, Paris, 1963*, eds. P. Grivet and N. Bloembergen (Dunod, Paris, 1964), Vol. 2, p. 1373.
48. J.M. Dawson, *Phys. Fluids* **7** (1964) 981.
49. P. Wägli and T.P. Donaldson, *Phys. Rev. Lett.* **40** (1976) 457; P. Lädrach and J.E. Balmer, *Opt. Commun.* **31** (1979) 350.
50. H. Hora, D. Pfirsch and A. Schlüter, *Z. Naturforsch.* **22A** (1967) 278.
51. H. Hora, *Phys. Fluids* **12** (1969) 81 and **17** (1974) 939.
52. J.W. Shearer, R.E. Kidder and J.W. Zink, *Bull. Am. Phys. Soc.* **19** (1970) 1483.
53. A. Zeidler, H. Schnabl and P. Mulser, *Phys. Fluids* **28** (1985) 372.
54. H. Hora, *Phys. Fluids* **28** (1985) 3706.
55. T. Rowlands, *Plasma Phys. & Controlled Fusion* **32** (1990) 297.
56. K.B. Büchl, K. Eidmann, P. Mulser, H. Salzmann and R. Sigel, *Laser Interaction and Related Plasma Phenomena*, eds. H. Schwarz and H. Hora (Plenum New York, 1972), Vol. 2, p. 503.
57. A. Wong and R. Stenzel, *Phys. Rev. Lett.* **34** (1975) 727; R. Stenzel, *Phys. Fluids* **19**, 865 (1976).
58. K. Försterling, *Arch. Elektron Ubertragungstech.* **5** (1950) 209.
59. W. Kruer, *Physics of Laser Plasma Interaction* (Addison-Wesley, Reading, Mass., 1986).
60. R.B. White and F.F. Chen, *Plasma Phys.* **16** (1974) 565.
61. H. Hora and A.K. Ghatak, *Phys. Rev.* **A31** (1985) 3473.
62. M.P. Goldsworthy, F. Green, P. Lalousis, R.J. Stening, S. Eliezer and H. Hora, *IEEE Trans. Plasma Sci.* **PS14** (1986) 823.
63. H. Hora, H. Haseroth, T. Henkelmann, C.E. Hill, G. Korschinek, R. Matulionienie and C.S. Taylor, *Analysis of Experiments on Energetic Ions from Laser Produced Plasmas with Reference to Hot Electrons and Pulsation*, CERN/PS/HI/Note 91-11.
64. T. Henkelmann, Diploma Thesis, Tech. Univ. Munich, 1990; T. Henkelmann, J. Sellmair and G. Korschinek, *Nucl. Instrum. Methods* **B56/57** (1991) 1152; G. Korschinek and T. Henkelmann, *Nucl. Instrum. Methods* **A302** (1991) 376.
65. Ingo Kunz, Dr. rer. nat. Thesis, Tech. Univ. Darmstadt, 1990.
66. R.Y. Chiao, E. Garmire and C.H. Townes, *Phys. Rev. Lett.* **13** (1964) 479.
67. H. Hora, *Z. Phys.* **226** (1969) 156.
68. F.F. Chen, *Laser Interaction and Related Plasma Phenomena*, eds. H. Schwarz and H. Hora (Plenum, New York, 1974), Vol. 3A, p. 291.
69. V.V. Korobkin and A.J. Alcock, *Phys. Rev. Lett.* **21** (1968) 1422.
70. M.C. Richardson and A.J. Alcock, *Appl. Phys. Lett.* **18** (1971) 357.
71. H. Hora, *J. Opt. Soc. Am.* **65** (1975) 882.
72. H. Hora and E.L. Kane, *Appl. Phys.* **13** (1977) 165.

73. T. Häuser, W. Scheid and H. Hora, *J. Opt. Soc. Am.* **B5** (1988) 2029; *Phys. Rev.* **A45** (1992) 1278.
74. D.A. Jones et al., *Appl. Phys.*, **B27** (1982) 157.
75. L.D. Landau, *J. Phys. USSR* **10** (1946) 25.
76. K.H. Spatschek, *Fortschr. Phy.* **27** (1977) 345.
77. W. Paul, *Rev. Mod. Phys.* **62** (1990) 531.
78. D. Biskamp and H. Welter, *Plasma Physics and Controlled Fusion Research, Tokyo, 1974* (IAEA, Vienna, 1975), Vol. 2, p. 507.
79. D. Bohm and E.P. Gross, *Phys. Rev.* **75** (1949) 1851.
80. D.F. Dubois, *Laser Interaction and Related Plasma Phenomena*, eds. H. Schwarz and H. Hora (Plenum, New York, 1974), Vol. 3A, p. 267.
81. S. Eliezer and H. Hora, Plasma Physics School, Varenna, ed. P. Caldriola (Soc. Fiz. Ital., Bologna, 1989), p. 375.
82. A.Y. Wong, *Laser Interaction and Related Plasma Phenomena*, eds. H. Schwarz and H. Hora (Plenum, New York, 1977), Vol. 4B, p. 783.
83. H.H. Chen and C.S. Liu, *Phys. Rev. Lett.* **37** (1976) 693; C.S. Liu and M.N. Rosenbluth, *Phys. Fluids* **17** (1974) 778; R. Dragila and H. Hora, *Phys. Fluids* **25** (1982) 1057.
84. C. Labaune et al. *Phys. Rev.* **A32** (1985) 577.
85. R.P. Drake, *Laser & Part. Beams* **6** (1988) 235.
86. I. Langmuir, *Phys. Rev.* **33** (1929) 954.
87. H. Alfvén, *Cosmic Plasmas* (Reidel, Dordrecht, 1981); *Laser & Part Beams* **6** (1988) 385.
88. C.-G. Fälthammer, *Laser & Part. Beams* **6** (1988) 437.
89. N. Hershkowitz, *Space Sci. Rev.* **41** 351 (1985).
90. J.A. Stamper, Laser & Part. Beams **9** (1991) 841.
91. P. Lalousis and H. Hora, *Laser & Part. Beams* **1** (1983) 283.
92. H. Hora, P. Lalousis and S. Eliezer, *Phys. Rev. Lett.* **53** (1984) 1650.
93. H. Hora, Gu Min, S. Eliezer, P. Lalousis, R.S. Pease and H. Szichman, *IEEE Trans. Plasma Sci.* **PS–17** (1989) 284.
94. K. Langbein, G. Riehl, H. Klein, K.N. Leung, S.R. Walther and R. Keller, *Rev. Sci. Instrum.* **61** (1990) 327; K. Langbein, GSI–90–29 (1990).
95. R.A.M. Maddever, B. Luther-Davies and R. Dragila, *Phys. Rev.* **A41** (1990) 2154.
96. J.H. Nuckolls, *Phys. Today* **35**, No. 9 (1982) 24.
97. M. Lubin, European Conference on Laser Interaction with Matter (ECLIM), Garching, April 1974.
98. M. Aydin and H. Hora, *Phys. Rev.* **A45** (1992) 6123.
99. A. Giulietti et al., *Laser Interaction with Plasmas*, eds. G. Velarde et al. (World Scientific, Singapore, 1989), p. 208.
100. A. Rode et al., Australian Institute of Nuclear Science and Engineering (AINSE) Conf., Feb. 1991.
101. K. Eidmann and R. Sigel, *Laser Interaction and Related Plasma Phenomena*, eds. H. Schwarz and H. Hora (Plenum, New York, 1974), Vol. 3B, p. 667.
102. R. Sigel, K. Eidmann, C.H. Pant and P. Sachsenmeis, *Phys. Rev. Lett.* **36** (1976) 1369.

103. Y. Kato et al., *Phys. Rev. Lett.* **53** (1984) 1057.
104. R.H. Lehmberg and S.P. Obenschain, *Opt. Commun.* **46** (1983) 27; R.H. Lehmberg, A.J. Schmitt and S.E. Bodner, *J. Appl. Phys.* **62** (1987) 2680.
105. Ximing Deng et al., *Appl. Opt.* **25** (1986) 377.
106. S. Skupski et al., *J. Appl. Phys.* **66** (1989) 3456.
107. P.J. Clark, S. Eliezer, F.J.M. Farley, M.P. Goldsworthy, F. Green, H. Hora, J.C. Kelly, P. Laousis, B. Luther-Davies, R.J. Stening and Wang Jin-Chen, *Laser Acceleration of Particles*, eds. C. Joshi and T. Katsouleas, AIP Proceedings No. 130 (AIP, New York, 1985), p. 380.
108. M. Siegrist, *J. Appl. Phys.* **88** (1977) 1375.